Six decades of the Hall–Petch effect – a survey of grain-size strengthening studies on pure metals

Citation: Cordero, Z. C. et al. "Six Decades of the Hall–Petch Effect – a Survey of Grain-Size Strengthening Studies on Pure Metals." International Materials Reviews 61, 8 (July 2016): 495–512 © 2016 Institute of Materials, Minerals and Mining and ASM International

As Published: https://doi.org/10.1080/09506608.2016.1191808

Publisher: Maney Publishing

Persistent URL: http://hdl.handle.net/1721.1/112642

Version: Author's final manuscript: final author's manuscript post peer review, without publisher's formatting or copy editing

Six Decades of the Hall-Petch Effect – A Survey of Grain-Size Strengthening Studies on Pure Metals

Authors: Zachary C. Cordero, Braden E. Knight, Christopher A. Schuh

Affiliations: Department of Materials Science and Engineering, MIT, Cambridge MA 02139

Corresponding Author: Prof. Christopher A. Schuh, schuh@mit.edu

Abstract: Refining a metal's grain size can result in dramatic increases in strength, and the magnitude of this strengthening increment can be estimated using the Hall-Petch equation. Since the Hall-Petch equation was proposed, there have been many experimental studies supporting its applicability to pure metals, intermetallics, and multi-phase alloys. In this article, we gather the grain size strengthening data from the Hall-Petch studies on pure metals and use this aggregated data to calculate best estimates of these metals' Hall-Petch parameters. We also use this aggregated data to re-evaluate the various models developed to physically support the Hall-Petch scaling.

Keywords: Hall-Petch, grain size strengthening, nanocrystalline metals, dislocations

1. Introduction

In the early 1950's, Hall[1] and Petch[2] empirically demonstrated that the initial yield point of low carbon steels, σ_y, was related to their grain size, D, according to the now well-known Hall-Petch relationship:

$$\sigma_y = \sigma_0 + k\frac{1}{\sqrt{D}} \quad (1)$$

where σ_0 and k are chemistry- and microstructure-dependent constants. In the six decades since Hall's and Petch's work, subsequent experimental studies have demonstrated that equation (1) or similar power laws apply not just to the initial yield of mild steels, but to the yield and flow stresses of other pure metals and alloys.[3] Despite the simplicity of equation (1) and its neglect of, e.g., crystallographic texture, other defect structures beyond grain boundaries, etc., it has proven remarkably relevant to metallurgy over that time. Because of such studies, grain-size strengthening data exists for most of the transition metals[4, 5] as well as pure Be,[6] Mg,[7] and Al.[8] And owing to the interest in nanocrystalline metals over the past two decades, for several of these metals there is now grain size strengthening data spanning six decades of grain size, from millimeter to nanometer-size grains.

In this article, we gather and assess grain size strengthening data for pure metals. Our two main motivations for this undertaking were the following. First, in the course of our own work on the design of nanocrystalline alloys, we felt the need for a reference compilation that could be used to estimate grain size strengthening effects in pure metals and alloys, and which could be more broadly useful to the mechanics of materials and microstructural design communities. Second, we wanted to encourage renewed discussion

of the possible mechanisms that give rise to power-law grain size strengthening such as equation (1) by comparing this aggregated grain size strengthening data with predictions from the many models that have been proposed to physically support equation (1).

Along these lines, this survey contains two main sections which address each of these goals in turn. In the first section, we present all of the currently available grain size strengthening data we have found in the open literature, and summarize best estimates of σ_0 and k for each of the pure metals that have been studied. Subsequently, we compare the trends seen in this aggregated grain size strengthening data with those predicted by the various theories explaining equation (1), starting with the pile-up model proposed by Hall in his original paper.[1, 9] We also briefly discuss the breakdown in the Hall-Petch scaling seen in the finest grain size nanocrystalline samples. The collection of many studies in a single analysis permits us to illustrate some effects of crystal structure, bond strength, temperature, and plastic strain on σ_0 and k that have not always been easily appreciated from individual studies.

2. Grain Size Strengthening Data

We summarize the BCC transition metals' grain size strengthening data in Figures 1a-g. In each of these Figures, we plot results from the various Hall-Petch studies on the different metals as well as best fits to the entirety of the data using equation (1). The open points indicate flow stresses measured using tension and compression tests while the closed points indicate Vickers and nanoindentation hardness measurements that were divided by a Tabor factor of 3 to convert to strength measurements. Figures 2 and 3 are formatted in the same way as Figure 1, but show data for the FCC and HCP metals, respectively. Most of the flow stresses included in Figures 1-3 were measured at plastic strains of order 0.2%, though some of the data points are from larger plastic strains, of order 1%, because those were the smallest strain values reported. The data in Figures 1-3 is provided in the supplementary material (Supplementary Material 1).

One prominent feature of Figures 1-3 is the scatter among the different studies' results. In many cases, this scatter can be ascribed to differences in sample preparation and testing methods. For example, studies on coarse-grained metals typically use specimens prepared by different thermomechanical processing techniques, e.g., swaging, rolling, or repeated upset forging, followed by recrystallization anneals. These different deformation processing techniques can produce distinct textures and, depending on the environment in which they are conducted, achieve different purities, both of which can have secondary effects on the grain-size strengthening behavior.[10, 11]

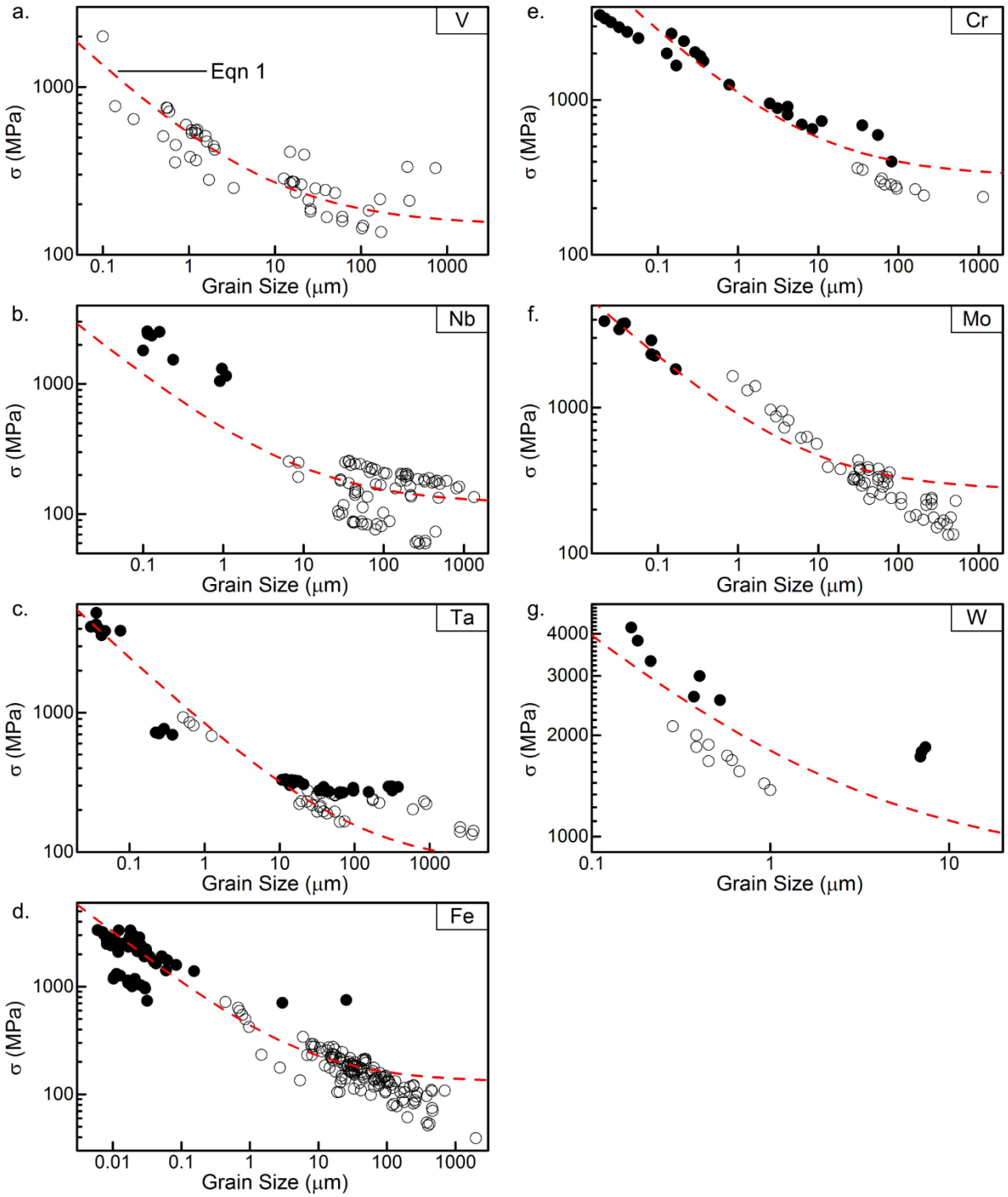

Figure 1: Aggregated Hall-Petch data for each of the BCC metals as well as best fits to the data using equation (1). The closed points indicate Vickers and nanoindentation hardness measurements that were divided by a Tabor factor of 3 while the open points indicate yield strengths measured using compression or tension tests. The Refs. included in a-g) are as follows: a) 12-18; b) 19-29; c) 14, 30-37; d) 38-56; e) 57-60; f) 61-66; and g) 67, 68.

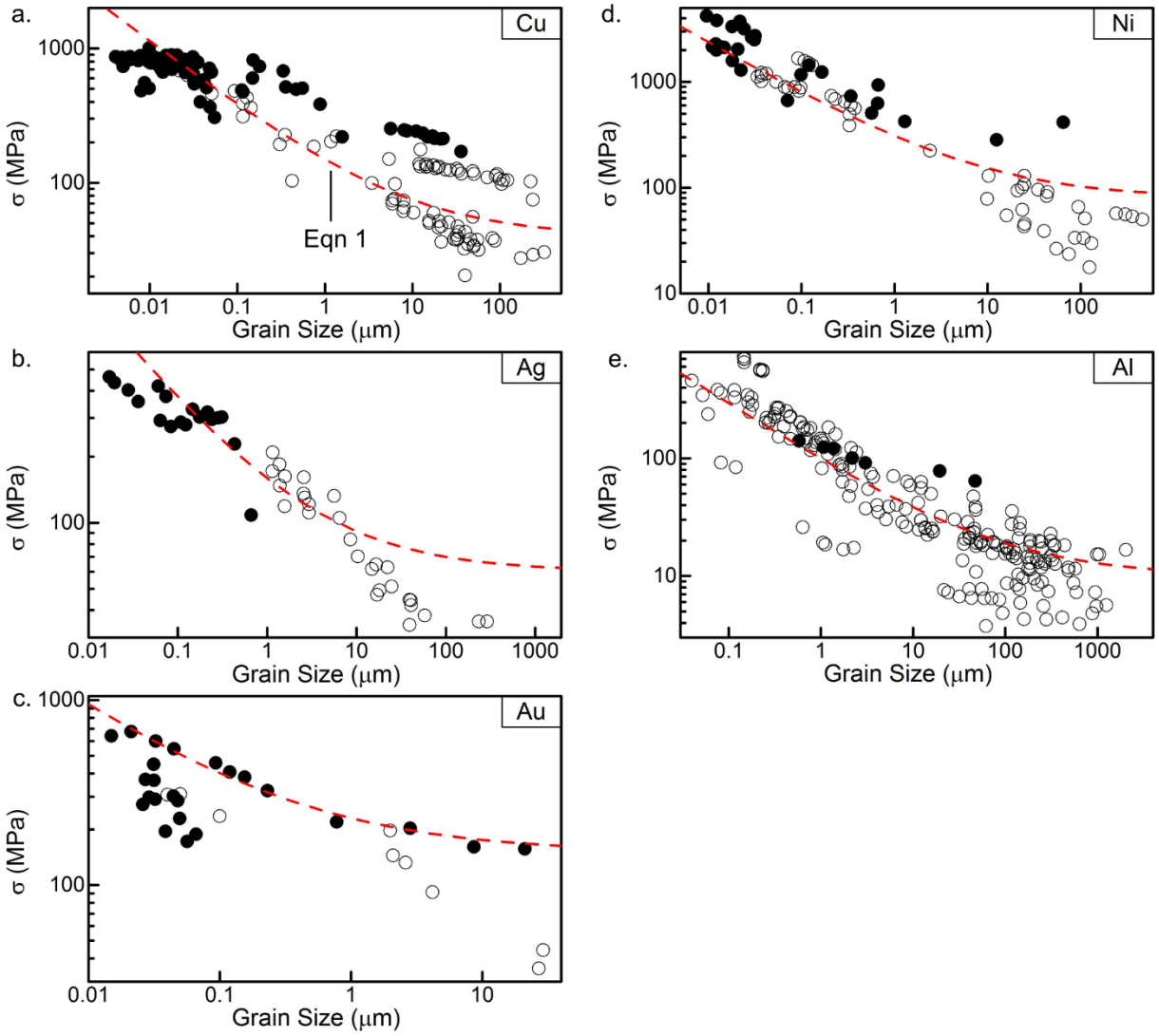

Figure 2: Aggregated Hall-Petch data for each of the FCC metals as well as best fits to the data using equation (1). The closed points indicate Vickers and nanoindentation hardness measurements that were divided by a Tabor factor of 3 while the open points indicate yield strengths measured using compression or tension tests. The Refs. included in a-e) are as follows: a) 69-86; b) 87-91; c) 92-95; d) 96-107; and e) 8, 108-122.

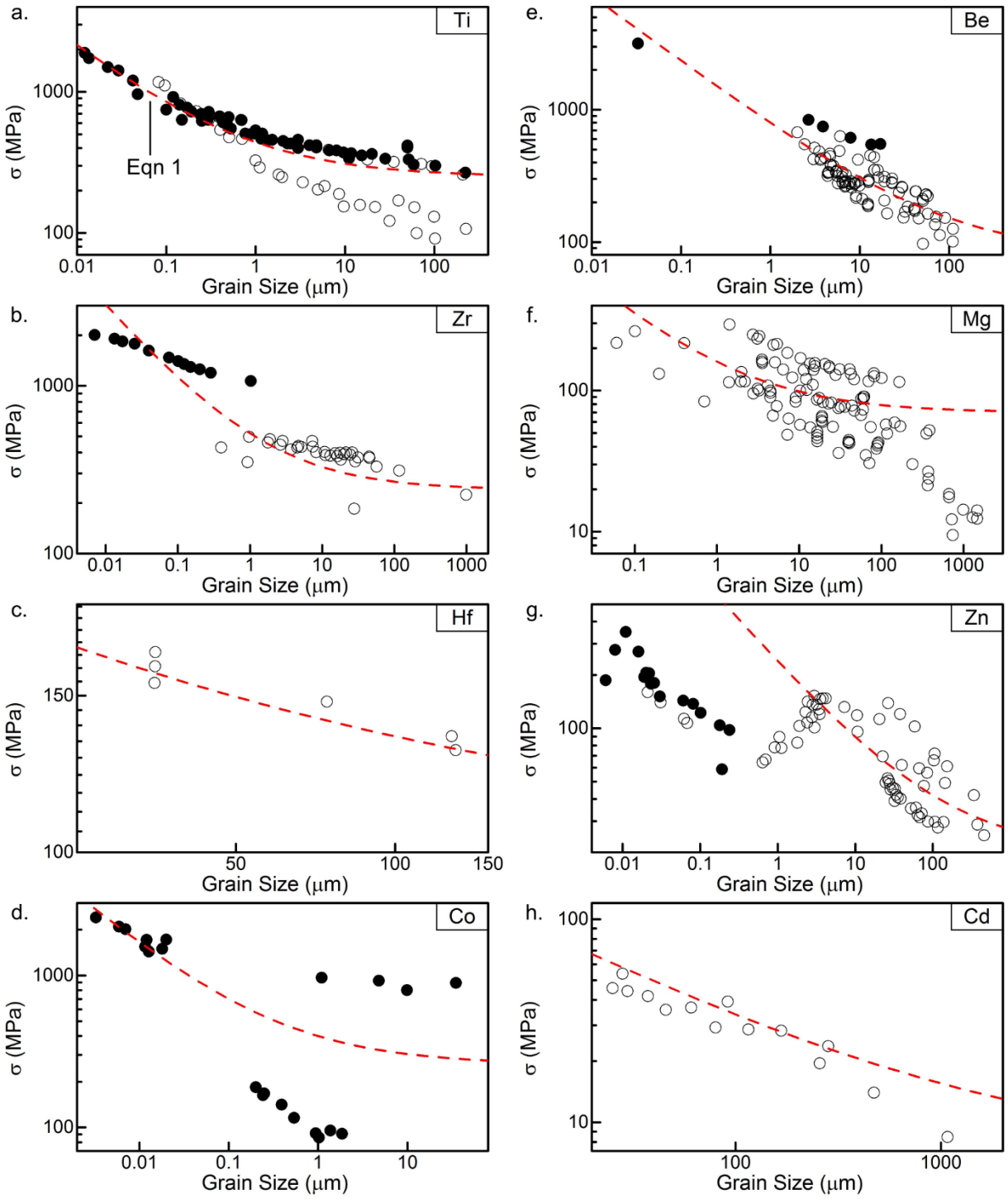

Figure 3: Aggregated Hall-Petch data for each of the HCP metals as well as best fits to the data using equation (1). The closed points indicate Vickers and nanoindentation hardness measurements that were divided by a Tabor factor of 3 while the open points indicate yield strengths measured using compression or tension tests. The Refs. included in a-h) are as follows: a) 123-132; b) 133-137; c) 138; d) 139-144; e) 6, 145-156; f) 7, 10, 157-163; g) 164-171; and h) 172-174.

Table 1 summarizes our best estimates of σ_0 and k at a plastic strain of order 0.2% for the metals included in Figures 1-3; metals absent from Table 1 have not been studied to the best of our knowledge or, as with Pd, do not appear to have sufficient, high-quality data. The σ_0 and k values are from best fits of equation (1) to the aggregated grain size strengthening data, with equal weighting to every data point from every study. We exercised some value judgments in this analysis, and specifically excluded data that had been questioned due to processing artefacts; this is especially the case for the finest grain sizes near the Hall-Petch breakdown where such artefacts are well known.[86, 175] The metals have been grouped by crystal structure and family in the periodic table. The range of grain sizes that have been investigated for each metal are also included in Table 1. Values of $Gb^{1/2}$ and $k/(Gb^{1/2})$, where G is the shear modulus and b is the Burgers vector, are listed in Table 1. The arithmetic mean and standard deviation of $k/(Gb^{1/2})$ for each crystal structure are shown as well.

Table 1: Summary of results from Hall-Petch studies on pure metals.

Crystal Struc.	Element	Group	D_{min} / D_{max} (μm)	σ_0 (MPa)	k (MPa μm$^{1/2}$)	Gb$^{1/2}$ (MPa μm$^{1/2}$)	k/(Gb$^{1/2}$) (–)	References
BCC	V	5	0.1 / 520	150	380	760	0.5	12-18
	Nb	5	0.1 / 610	120	340	630	0.5	19-29
	Ta	5	0.04 / 3900	80	760	1170	0.7	14, 30-37
	Cr	6	0.02 / 1100	320	800	1820	0.4	57, 59, 60
	Mo	6	0.02 / 511	270	630	2070	0.3	61-66
	W	6	0.16 / 7	800	1000	2660	0.4	67, 68
	Fe	8	0.009 / 2000	130	310	1290	0.2	38-44, 47, 49-56
						MEAN	0.42 ± 0.07	
FCC	Ni	10	0.01 / 460	80	230	1200	0.2	96-104, 106
	Cu	11	0.005 / 320	40	110	770	0.1	69, 70, 72, 73, 75, 76, 78, 85
	Ag	11	0.01 / 250	60	100	500	0.2	87, 88
	Au	11	0.02 / 200	150	80	440	0.2	92
	Al	13	0.08 / 1200	10	90	440	0.2	8, 108-122
						MEAN	0.18 ± 0.02	
HCP	Be	2	0.03 / 1100	80	720	680	1.1	6, 145-154, 156
	Mg	2	0.2 / 1000	70	90	100	0.9	10, 157-163
	Ti	4	0.01 / 250	250	190	640	0.3	123-126, 128-132
	Zr	4	0.4 / 1000	240	280	210	1.3	133-135
	Hf	4	35 / 130	100	350	320	1.1	138
	Co	9	0.012 / 4.8	260	140	380	0.4	139-144
	Zn	12	0.02 / 500	20	220	230	1.0	164, 165, 168, 171
	Cd	12	28 / 1080	7	220	150	1.5	172-174
						MEAN	0.9 ± 0.2	

3. Models for Grain Size Strengthening

We now turn our attention to the theoretical underpinnings of equation (1). Table 2 summarizes various different models that have been proposed to explain equation (1) and the data presented in Figures 1-3. Most of these models treat the two terms on the right hand side of equation (1) separately: the physics associated with grain size strengthening is assumed to be encoded in *k* and the grain size exponent in the second term, while σ_0 is taken to account for all strengthening effects unrelated to the grain size.

Table 2: Summary of grain size strengthening models.

Model		Year	Equation	Physics
Pile-up	Hall[1]	1951	equation (1)	Grain boundaries (GBs) are obstacles preventing dislocation motion. Dislocations emit into adjacent grains when the shear stress at the head of a dislocation pile-up reaches some threshold value.
	Petch[2]	1953	equation (1)	Same as above.
	Cottrell[176]	1958	$\sigma = \sigma_0 + \tau_d \sqrt{\frac{l}{D}}$ l = distance from GB to source τ_d = unpinning stress	Stresses generated by dislocation pile-ups in one grain activate Frank-Read sources in adjacent grains.
	Armstrong et al.[164]	1962	$\sigma = \sigma_0 + \tau_d m^2 \sqrt{\frac{l}{D}}$ m = Taylor orientation factor	Similar model to Cottrell's but accounts for the fact that the dislocation source might be on a different slip system than that of the dislocation pile-up. Accounts for the effect of crystal structure on *k* through the Taylor factor, *m*.
	Smith and Worthington[177]	1964	$\sigma = \sigma_0 + \tau_d m_1 m_2 \sqrt{\frac{l}{D}}$ m_1 = macro-orientation factor m_2 = micro-orientation factor	Modified version of Armstrong's model. It can account for the effect of microtexture on the activation of dislocation sources.
	Navarro and de los Rios[178]	1988	$\sigma = \sigma_0 + \frac{2\tau_d m^2}{\pi} \sqrt{\frac{l'}{D}}$ l' = "effective position" of source	Similar model to Cottrell's but the dislocation source is assumed to extend over a finite distance.
	Nazarov[179]	1996	See Ref. 179, equation (30).	GB film preventing dislocation motion is broken down when the shear stress at the head of a dislocation pile-up reaches some threshold value. After yielding, dislocations accumulate in the GB and strongly affect the strength of the GB film.
	Friedman and Chrzan[180]	1998	$\sigma = \sigma_0 + \sqrt{\tau_d^2 + \frac{Gb\chi}{\pi D}}$ χ = constant	Similar to the Cottrell model but dislocations can exert backstresses that make it more difficult for Frank-Read sources to operate.
GB source	Li[181]	1963	$\sigma = \sigma_0 + \alpha G b \sqrt{\frac{3s}{D}}$	Dislocations generated from GBs at yielding strengthen the material through the Taylor equation. The density of dislocations generated at yielding is proportional to the GB area because the dislocations are generated at GB ledges.

			s = line length of dislocation emitted per unit area of grain boundary α = material-dependent constant of order unity	
	Bata and Pereloma[182]	2004	See Ref. 182, equation (32)	Grain size strengthening arises because of the work required to eject dislocations from GBs. Does not rely on the Taylor equation. See comments by Wert[183] and Gavriljuk[184].
GND	Ashby[185]	1970	$\sigma = \sigma_0 + CG\sqrt{\frac{b\varepsilon}{D}}$ C = material-dependent constant	Compatible deformation of individual grains in a polycrystal requires the introduction of geometrically necessary dislocations (GND's). Density of GND's is inversely proportional to the grain size. GND's affect the strength through the Taylor equation.
Composite	Thompson et al.[186]	1973	$\sigma = \sigma_0 + \left(1 - \frac{\lambda_S}{D}\right)\left(\frac{K_1}{D}\right) + \frac{\lambda_S}{D}\sqrt{\frac{K_2}{D}}$ λ_S = statistical slip length K_1, K_2 = constants	Treat the individual grains as composites with different dislocation densities in the grain interior and the region near the grain boundary. Dislocations affect the strength through the Taylor equation. The macroscopic flow stress is the area average stress of the two regions.
	Meyers and Ashworth[187]	1982	See Ref. 187, equation (33)	Elastic incompatibility leads to the generation of dislocations near the grain boundary at small strains. Treat grains at yielding as a composite with a work-hardened layer near the grain boundary.
Slip distance	Conrad[188]	1963	$\sigma = \sigma_0 + \alpha G\sqrt{\frac{b\varepsilon}{\sqrt{D}}}$ ε = strain	Assumes that the grain size affects the dislocation density, which affects the strength through the Taylor equation; that dislocations are not annihilated during the early stages of plastic straining; and that the dislocation slip distance is proportional to square root of the grain size.
	Conrad et al.[29]	1967	$\sigma \approx \sigma_0 + \alpha G\sqrt{\frac{b\varepsilon}{D}}$	Similar to Conrad's earlier model but assumes the slip distance is proportional to the grain size, not its square root.
	Meakin and Petch[189]	1974	$\sigma = \sigma_0 + \theta m^2 G\varepsilon + \tau_a m^2\sqrt{\frac{l}{D}} + \alpha m^{3/2} G\sqrt{\frac{b\varepsilon}{D}}$ θ = material-dependent constant	Combines the traditional pile-up model with the slip distance model due to Conrad.

Hall's explanation of the grain size strengthening term in equation (1) relied on the concept of a dislocation pile-up against a grain boundary.[1] According to his model, dislocations pile up at grain boundaries in one grain and macroscopic yielding occurs when dislocations are emitted into the adjacent grain. This is possible when the sum of the external stress and the stress at the head of the dislocation pile-up is larger than some threshold stress. The strength depends on grain size because the total pile-up length is limited by the grain size, which therefore limits the stress at the head of the pile-up. As a result, the pile-up model predicts a linear relationship between the yield stress and the reciprocal square root of the grain size. There are many variations on this same basic model that are summarized in a review by Li and Chou,[9] but they all give a grain size strengthening equation of the same basic form

$$\sigma = \sigma_0 + \beta G b^{1/2} D^{-1/2} \quad (2)$$

where b is the magnitude of the Burgers vector, β is a model-dependent constant that is typically on the order of 0.1, and the pre-factor $\beta G b^{1/2}$ is equivalent to k from equation (1); the values of $k/(Gb^{1/2})$ given in Table 1 correspond to β. The best fit results for the compiled data show that β is between 0.1 and 0.7 for the cubic metals, which is the same order of magnitude as predicted by the pile-up model. The data also show that β depends on crystal structure (being on average 0.18 for FCC, 0.42 for BCC, and 0.9 for HCP metals) and Armstrong et al. demonstrated that the pile-up model can be modified to account for this.[164]

Despite these successes, the pile-up model nonetheless suffers from several major deficiencies, the most important of which is the lack of direct evidence relating the dislocation pile-up length to the grain size.[9, 190] In addition, the pile-up mechanism cannot account for k's sensitivity to the average grain boundary structure and chemistry, which was demonstrated by Floreen and Westbrook in experiments on sulphur-doped nickel.[96] These issues with the pile-up model motivated the development of an alternative class of work-hardening models that assume grain boundaries influence the dislocation density, ρ, which in turn affects the flow stress through the Taylor equation:

$$\sigma = \sigma_0 + \alpha G b \sqrt{\rho} \quad (3)$$

where α is a material-dependent constant.

The first of these work-hardening models, developed by Li, is based on the idea of grain boundary ledges that can serve as dislocation sources at yielding.[181] Li proposed that the density of these ledges scales with the grain boundary area per unit volume of material. As a result, more dislocation line length, and hence greater dislocation densities, are generated in fine grained materials when they yield. Li showed how this mechanism can give a grain size strengthening relationship with the same functional form as equation (1), but as with the pile up model, there is no direct evidence linking the density of grain boundary ledges to that of dislocations.

Ashby's theory of grain size strengthening is another work-hardening model, but it differs from the grain boundary ledge model in that it tries to explain equation (1) by reconciling two sets of observations instead of speculating about a specific mechanism. The first set of observations is that ρ increases linearly with plastic strain and inverse grain size during the uniform deformation of polycrystalline iron,[38, 191] vanadium,[192] titanium,[123] niobium,[29] and aluminium.[108] The second set of observations is that even when a polycrystalline specimen is subjected to macroscopically uniform plastic deformation, the individual grains still exhibit non-homogeneous plastic flow.[4, 193, 194] This non-uniform plastic flow is due to compatibility constraints at grain boundaries, which result in the activation of additional slip systems and the generation of excess dislocations near grain boundaries.[195] In the absence of such constraints, the individual grains in a polycrystal would simply shear on their glide planes with the largest critically resolved shear stresses.

Ashby showed that these two sets of observations are in fact related by envisioning the deformation of a tensile specimen as a two-step process.[185] In the first step, the grains undergo unconstrained, uniform deformation by shearing along their glide planes with the largest resolved shear stresses. During this first step, dislocations accumulate through random trapping events just as in a uniformly strained single crystal. The density of this group of dislocations, ρ_{SS}, is influenced by the same material and testing parameters that affect the dislocation density in a plastically strained single crystal, such as crystal structure, stacking fault energy, and homologous temperature. Since compatibility is not enforced during this first step, voids and overlaps develop between adjacent grains, and the total amount of these defects per grain is proportional to $D^2\varepsilon/2$ where ε is the macroscopic plastic strain. In the second step, these voids and overlaps are removed by introducing dislocation arrays next to the grain boundaries. The total dislocation line length that must be generated in each grain to restore compatibility is approximately $D^2\varepsilon/4b$. Because the average volume per grain is proportional to D^3, the density of this second set of dislocation is

$$\rho_{GN} \approx \varepsilon/4Db. \quad (4)$$

This relationship has the same strain and grain size dependencies seen in experiments. Note that this second set of dislocations is only introduced to ensure compatibility, so its density, to first order, is unaffected by the material and testing parameters listed above.

Ashby next showed how his model could explain the Hall-Petch equation by combining his predictions about the strain and grain-size dependence of the dislocation density with the Taylor hardening equation. Assuming for simplicity that the two groups of dislocations do not interact, the total dislocation density is $\rho = \rho_{GN} + \rho_{SS}$. Inserting this cumulative dislocation density into equation (3) gives

$$\sigma = \sigma_0 + \alpha G b\sqrt{\rho_{GN} + \rho_{SS}} \quad (5)$$

which can be rewritten as

$$\sigma \approx \sigma_0 + \alpha G\sqrt{b\varepsilon/4D} \quad (6)$$

when $\rho_{GN} \gg \rho_{SS}$, as is likely the case for small plastic strains.

Comparing equations (1) and (6), we see that Ashby's model gives the correct reciprocal square root dependence on grain size, but now the Hall-Petch coefficient also depends on plastic strain, $k \propto \sqrt{\varepsilon}$. To test for this parabolic strain-dependence, several investigators have measured *k* as a function of plastic strain, and the results from these studies are shown in Figures 4a-c. Here, the *k* values have been normalized by $Gb^{1/2}$ for comparison purposes.

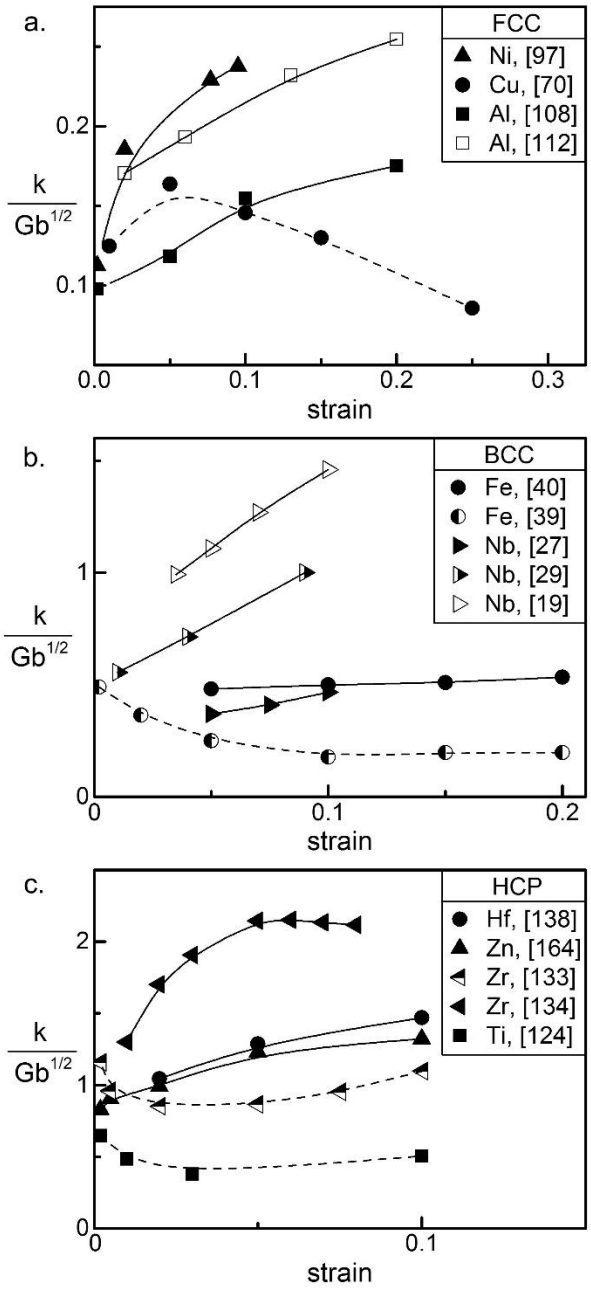

Figure 4: k/(Gb$^{1/2}$) as a function of plastic strain for several FCC, BCC, and HCP metals.

In most of the studies shown in Figures 4a-c, *k* increased with plastic strain, though there are some few anomalous studies in which *k* decreased with plastic strain. These include studies of the HCP metals titanium and zirconium,[124, 133] FCC copper,[70, 85] as well as BCC iron.[39] The *k* values of titanium and zirconium exhibit a similar trend, first decreasing and then slightly increasing with plastic strain. The most likely explanation for this initial sharp decrease in *k* is that these metals deform by twinning at small plastic strains and by dislocation glide at larger plastic strains. This results in an apparent decrease in *k* because a metal typically has a larger Hall-Petch coefficient when it deforms by twinning than when it deforms by dislocation glide, as shown by Marcinkowski and Lipsitt.[59] The strain-dependence of copper's *k* is the reverse of titanium's and zirconium's: its *k* initially increases and then decreases with plastic strain. Ono and Karashima directly linked this behavior to the fiber-texture that can develop in recrystallized copper samples by performing tension tests on textured and texture-free samples.[70] Finally, Jago and Hansen found that iron's *k* decreases monotonically with plastic strain; however, these results have been contradicted by another study that showed iron's *k* to increase slightly with plastic strain.[39, 40]

Thus, consistent with Ashby's equation (6), the Hall-Petch coefficients of most metals increase with plastic strain, and for the studies that appear to contradict Ashby's predictions, there are either physical explanations or counterexamples. Despite this qualitative agreement between experiments and Ashby's theory, none of the results in Figures 4a-c exhibit the parabolic dependence on strain predicted by Ashby. Instead, non-linear fits to the data in Figures 4a-c suggest that the strain exponent in equation (6) is closer to ~0.2. One possible reason for this discrepancy is that the strains at which *k* have historically been measured are so large that the assumption $\rho_{GN} \gg \rho_{SS}$ is no longer valid.

Many of the more recent models of grain size strengthening listed in Table 2 are based on Ashby's concept of geometrically necessary dislocations.[186, 187, 196, 197] These models treat the individual grains as composites with grain boundary and grain interior regions that accumulate dislocations at different rates and have different strengths as a result. Typically, the macroscopic yield strength in these models is the average strength of these two regions.

Finally, the mean slip distance model, proposed by several investigators,[29, 188, 189] arrives at a relationship similar to equation (6) and predicts many of the same behaviors as Ashby's framework, but it relies on a different set of assumptions: (1) that the average dislocation slip distance, L_{ave}, is proportional to the grain size, $L_{ave} = \eta D$, and (2) that the dislocations generated during straining do not annihilate one another. This second assumption allows the Orowan equation to be written as follows

$$\rho = \varepsilon / L_{ave} b = \varepsilon / \eta D b. \quad (7)$$

Combining equations (3) and (7) gives the following grain size strengthening relationship

$$\sigma = \sigma_0 + \alpha G\sqrt{\varepsilon b/\eta D} \quad (8)$$

with $k = \alpha G\sqrt{\varepsilon b/\eta}$, similarly to the Ashby model. The heterogeneous dislocation substructures seen in plastically deformed polycrystals seem to support the Ashby model over the mean slip distance model.[190, 198]

All of the models described thus far predict a reciprocal square root dependence on grain size, in agreement with the classic Hall-Petch equation; however, several investigators have suggested that the grain-size exponent should be something other than -1/2.[188, 199-204] For example, Christman fitted experimental grain-size strengthening data using a power law of the form

$$\sigma = \sigma_0 + kD^n \quad (9)$$

where n, σ_0, and k were all fitting parameters, and found that n was -1/3 for the FCC metals and varied between -1/2 and -0.9 for the BCC metals.[200] Christman did not provide a physical explanation for these alternate grain size dependences, but other researchers have. In an early version of the mean slip distance model, for instance, Conrad proposed that the mean slip distance had a parabolic dependence on the grain size, which gives n = -1/4 when combined with equations (3) and (7).[188] Kocks[204] and Hirth[201] both described a composite model for which n = -1. And most recently, Dunstan and Bushby argued that n = -1 because the stress required to move a dislocation is related to its radius of curvature, which is limited by the grain size in a polycrystal.[202]

To identify the grain size exponent that best describes the experimental results, we fitted equation (9) to each metal's aggregated grain size strengthening data. We used a special fitting procedure to account for σ_0's sensitivity to differences in specimen preparation and characterization, which vary widely among the different studies: For a given metal, we fitted equation (9) to the results from each individual study, and treated n and k as global parameters that were same for all of the fits, and σ_0 as a local parameter that could be different for each fit. This procedure gives results like those shown in Figure 5, which presents the grain size strengthening data for Ni alongside the fits to the individual datasets. Each of these curves was calculated using the same values of n (-0.39) and k (330 MPa $\mu m^{0.39}$), but a different value of σ_0, which is why they are displaced from one another. We used this fitting procedure to calculate values of k and n for each of the metals, and the results are summarized in Table 3. Table 3 shows that while the n values range from -0.03 (Hf) to -0.95 (W), the average value is -0.40±0.05, which seems to support the classic Hall-Petch scaling, n = -1/2, over the n = -1 scaling that has been proposed by other investigators.[201-204] In general, the largest deviations tend to be from materials for which data is more scarce or spans a more limited range of grain sizes, with three notable exceptions – Fe, Zn, and Mg. There also appear to be slight, systematic differences between the average n values for the BCC (n_{ave} = -0.52 ± 0.09), FCC (n_{ave} = -0.40 ±

0.08), and HCP metals (n_{ave} = -0.29 ± 0.07), in line with Christman's observations. Certainly this discussion serves to highlight the need for more work examining the generality of the exponent.

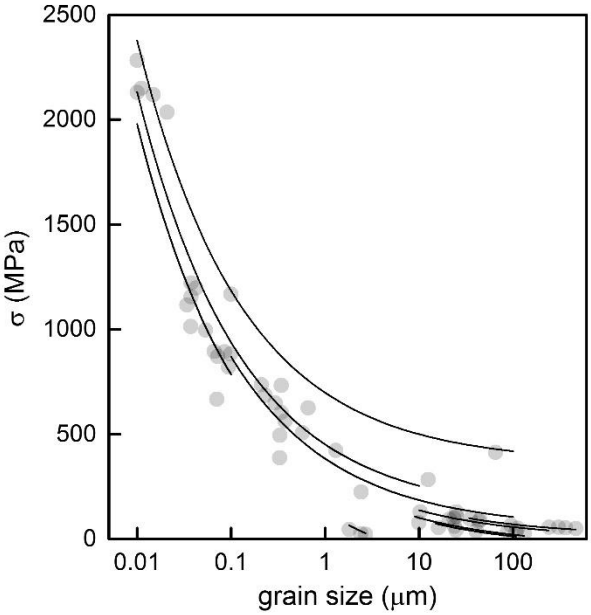

Figure 5: Aggregated grain size strengthening data for Ni as well as best fits using equation (9) to the results from the individual studies.

Table 3: *n* and *k* values from best fits using equation (9) to each metal's aggregated grain size strengthening data.

	n	k (MPa μm^{-n})
V	-0.47	280
Nb	-0.54	500
Ta	-0.54	260
Cr	-0.58	650
Mo	-0.32	1420
W	-0.95	410
Fe	-0.29	640
Ni	-0.39	330
Cu	-0.38	160
Ag	-0.17	300
Au	-0.47	100
Al	-0.60	100
Be	-0.56	870
Mg	-0.21	150
Ti	-0.47	210
Zr	-0.19	540
Hf	-0.03	800
Co	-0.51	100
Zn	-0.15	80

Cd	-0.17	190

The models described above explain how the grain size affects the strength, but much of the scatter in Figures 1-3 is probably due to strengthening contributions that are not directly related to grain size. These other strengthening increments are nominally included in the frictional stress, σ_0, and below room temperature, the terms that make up σ_0 in a pure metal can be separated into two categories: temperature-dependent and athermal. The temperature-dependent component of σ_0 includes the Peierls-Nabarro stress, which is negligible for FCC and HCP metals, but can be quite large for BCC metals.[205, 206] The athermal components of σ_0 include solid solution strengthening and work hardening. We consider work hardening as approximately athermal because the strengthening increment from a given dislocation substructure is nearly independent of temperature.

The contributions of the Peierls-Nabarro stress, solid solution strengthening, and work hardening to σ_0 are typically assumed to be independent and additive:[207]

$$\sigma_0 = \sigma_{0,PN} + \sigma_{0,SS} + \sigma_{0,WH}. \quad (10)$$

Here the subscripts *PN*, *SS*, and *WH* refer to Peierls-Nabarro, solid solution, and work-hardening, respectively. In addition, each strengthening mechanism's contribution to σ_0 is approximately proportional to its contribution to the critical resolved shear stress of a single crystal:

$$\sigma_{0,PN} \approx M_{ave}\tau_{0,PN}$$
$$\sigma_{0,SS} \approx M_{ave}\tau_{0,SS} \quad (11a\text{-}c)$$
$$\sigma_{0,WH} \approx M_{ave}\tau_{0,WH}$$

where $\tau_{0,PN}$, $\tau_{0,SS}$, and $\tau_{0,WH}$ are the respective strengthening increments in a single crystal from the Peierls-Nabarro stress, solid solution strengthening, and work hardening, and M_{ave} is the Taylor factor.[41, 42, 59, 108, 164] The Taylor factor accounts for the homogeneous deformation of the individual grains in a polycrystal.[208]

We can evaluate the validity of equations (11a-c) by comparing the temperature and strain dependencies of σ_0 with those of single crystal yield and flow stresses. For instance, Figure 6a, taken from the work by Marcinkowski and Lipsitt,[59] shows the σ_0 and $M_{ave}\tau_0$ of Fe as a function of temperature at constant strain, and illustrates how the datasets are very similar in magnitude and form, in line with equation (11a). In Figures 6b-e, we repeat the Marcinowski-Lipsitt analysis for several other BCC metals, plotting the σ_0 and $M_{ave}\tau_0$ as a function of temperature at constant strain, and demonstrate that equation (11a) applies to these other metals as well. The outlying points in Figure 6 can be explained when we account for differences in sample purity and the contribution of solid solution strengthening to σ_0. For example, in Figure 6d, solid

solution strengthening due to the large C concentration (1000 ppm) in Lindley and Smallman's vanadium specimens resulted in the 250 MPa offset of their results relative to the other measurements.[12]

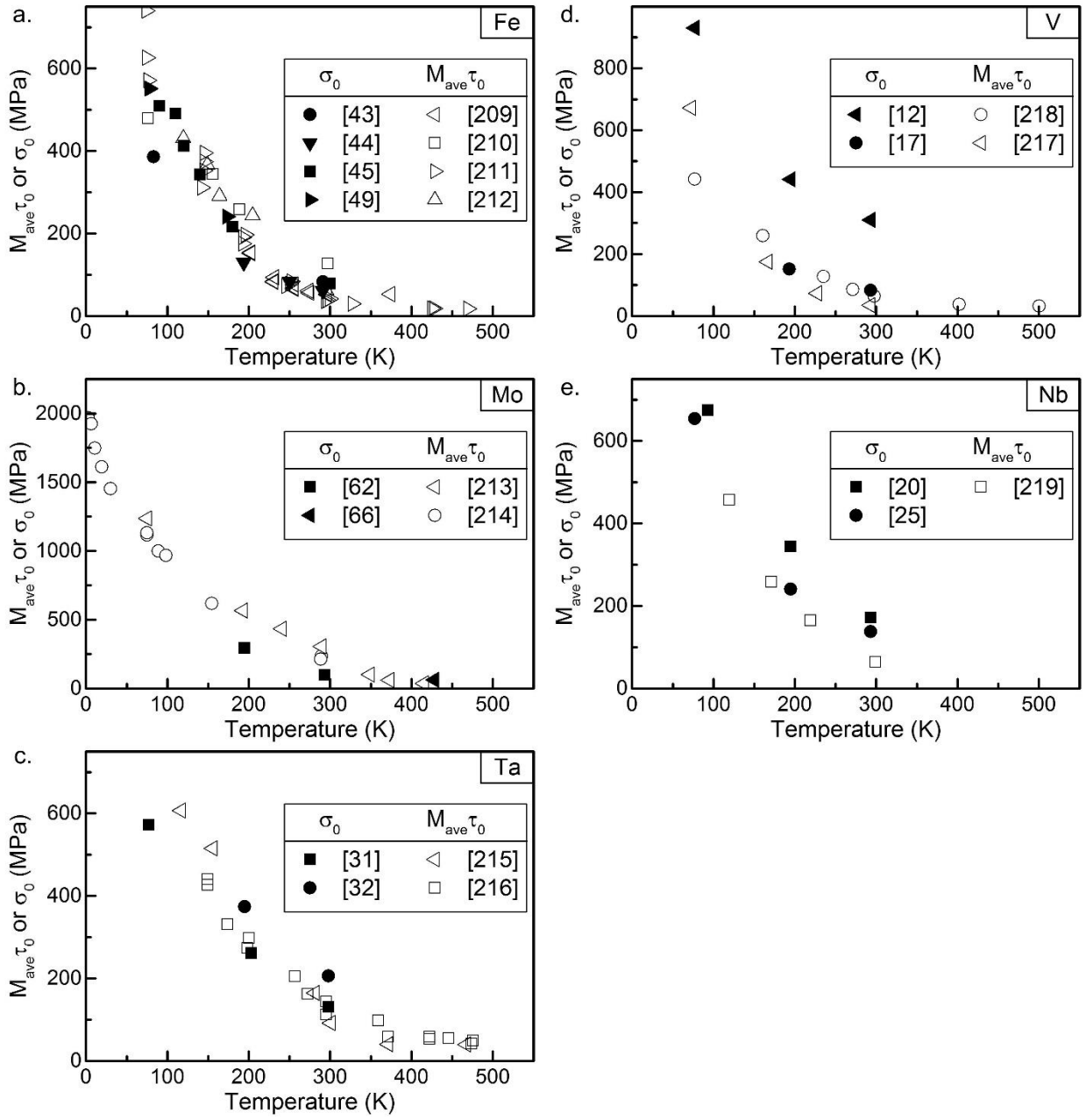

Figure 6: Testing temperature versus $M_{ave}\tau_0$ from tension tests on single crystals and σ_0 from fits to yield stress measurements using the Hall-Petch equation. We used M_{ave} = 2.7 which is appropriate for BCC polycrystals that exhibit pencil glide and have no texture.[208] The close correspondence between $M_{ave}\tau_0$ and σ_0 supports equation (11a). The large and rapid increase in both $M_{ave}\tau_0$ and σ_0 with decreasing temperature reflects the BCC metals' large, temperature-sensitive Peierls-Nabarro stress. The single crystal data in a-e) are from the following Refs.: a) 209-212; b) 213, 214; c) 215, 216; d) 217, 218; and e) 219.

Figure 6 only shows data for BCC metals, as the FCC and HCP metals do not have nearly as significant a volume of data to examine. Nonetheless, FCC metals tend to exhibit the same trends, except the effect of temperature is much less dramatic than it is for BCC metals, which is expected given FCC metals' generally weaker Peierls-Nabarro stresses. On average, the σ_0 and $M_{ave}\tau_0$ of FCC metals increase at most just a few dozen MPa on cooling from room temperature to 77 K.[70, 71, 97, 109] The HCP metals behave similarly to the FCC metals, aside from anomalous reports of large increases in Zr's σ_0 on cooling by Coleman and Hardie[133] and Ramani and Rodriguez,[134] which may have been due to the onset of deformation twinning.

Following Hansen,[108] we illustrate the contribution of work-hardening to σ_0 by plotting plastic strain against σ_0/G, where G is the shear modulus, in Figures 7a-c. In line with equation (11c), the increase in σ_0/G with plastic strain seen in these Figures resembles the increase in τ_0/G due to work-hardening during the axisymmetric deformation of single crystals.[220] This effect of plastic strain on σ_0/G was first observed in early Hall-Petch studies;[71, 108] however, in the context of the present larger dataset, new trends in the plastic strain dependence of σ_0/G become apparent. For example, closer inspection of Figures 7a-c reveals that material and testing parameters affect work hardening's contribution to σ_0/G in the same way they influence its contribution to τ_0/G. Comparison of Figures 7a and 7b shows that σ_0/G increases more rapidly with plastic strain in FCC metals than it does in BCC metals. This is consistent with FCC single crystals' much greater normalized rates of work hardening than BCC or HCP single crystals'.[221] Figure 7b shows that FCC metals with smaller stacking fault energies exhibit greater increases in σ_0/G at a given strain. Comparing the results from tests performed at 77 K shown in Figure 7c with those in Figure 7b demonstrates that plastically straining at lower testing temperatures can result in larger increases in σ_0/G at a given strain. These last two trends are evident in tests on FCC single crystals as well, where lower stacking fault energies and testing temperatures are known to increase the rate of work hardening by suppressing dynamic recovery.[221, 222]

The similar strain dependencies of σ_0/G and τ_0/G support Ashby's argument that dislocations can be divided into two groups. One group consists of the statistically stored dislocations that contribute to changes in σ_0/G. The density of these dislocations at a given strain is comparable to the dislocation density of a single crystal subjected to the same amount of uniform deformation and is strongly affected by variables such as crystal structure, stacking fault energy, and temperature (cf. Figure 6). The second group of dislocations contains the excess dislocations that ensure the compatible deformation of the individual grains in a polycrystal. And in the context of the Ashby model, it is this second group that gives rise to grain size strengthening.

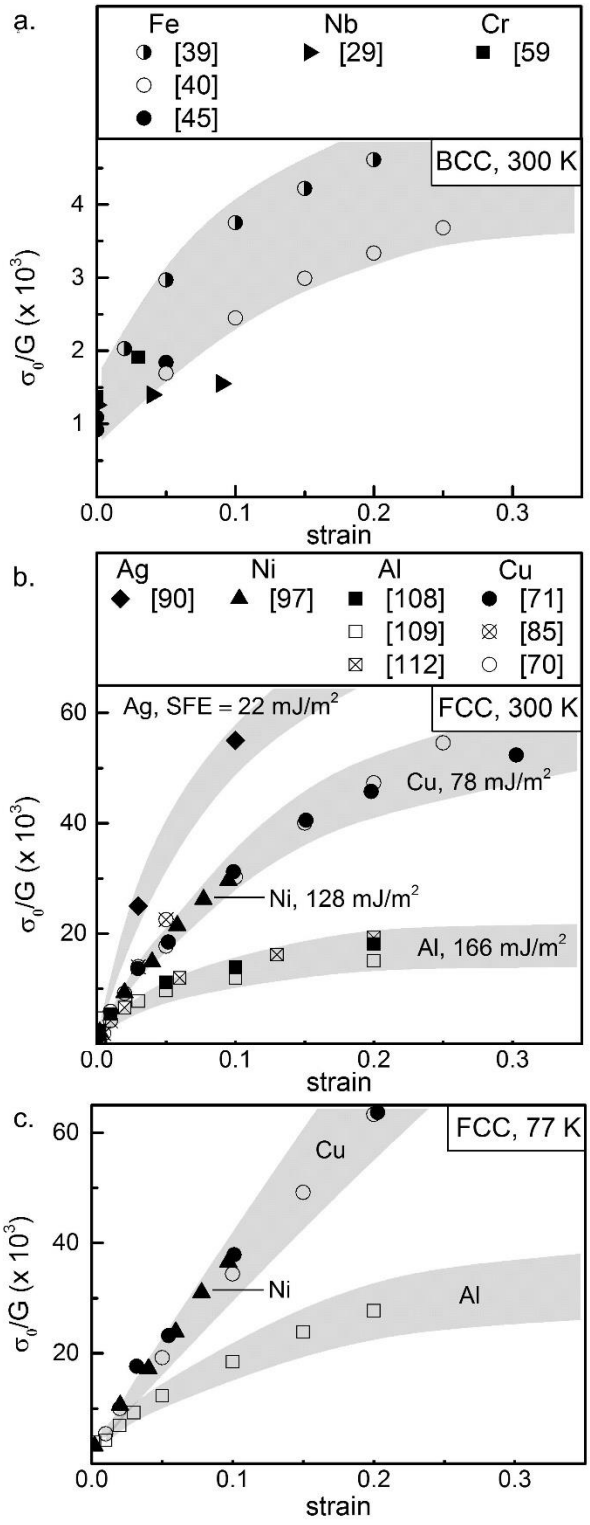

Figure 7: a) Increase in several BCC metals' σ_0/G with plastic strain at room temperature. b,c) Increase in several FCC metals' σ_0/G with plastic strain at room temperature and 77 K, respectively. Note the close resemblance of these results to the increase in the flow stress of single crystal test specimens oriented for multislip during tension or compression testing. The material and testing parameters affecting the

normalized rate of work-hardening of single crystals – crystal structure, stacking fault energy (SFE),[223] temperature – have the same effect on σ_0/G's strain dependence.

Returning now to the aggregated grain size strengthening results shown earlier, we can use the concepts just introduced to explain much of the scatter seen in this data. As an example, consider Figure 8 which shows fits using equation (1) to the niobium yield stress data from Refs. 19, 20, 23, 24, 27, 29. The large offsets between the fits in this figure are primarily due to solid solution strengthening from interstitial contaminants whose concentration varied from study to study. To demonstrate this, in Table 4 we compare each study's σ_0 with the expected solid solution strengthening increment due to their specimens' oxygen and nitrogen contents, σ_{SS}. As Table 4 shows, Ref. 27's samples had the smallest solid solution strengthening increment, which is why their σ_0 is the smallest and their results sit well below the others in Figure 8. By comparison, the other studies used relatively impure samples, and the values in Table 4 show that for several of these other studies, their predicted solid solution strengthening increments can account for the difference between their σ_0 and Ref. 27's.

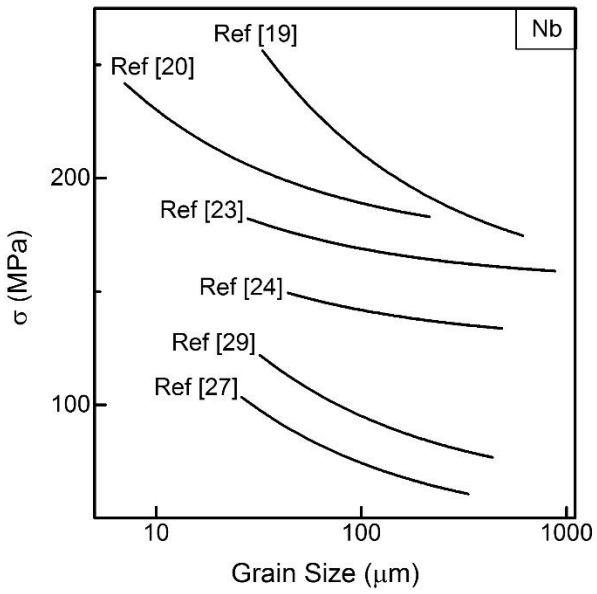

Figure 8: Independent fits using equation (1) to the niobium grain size strengthening data from Refs. 19, 20, 23, 24, 27, 29.

Work-hardening is not important in Figure 8 because the niobium results were all measured at the same plastic strain, but it does contribute to the scatter in chromium's grain size strengthening data shown in Figure 9. Here the hardness measurements from Ref. 60 are offset ~200 MPa above the yield strength measurements from Ref. 59, and this is because hardness measurements include some plastic strain. Following Tabor, the Vickers hardness is equal to the flow stress of a test specimen after it has been plastically strained an additional 8%.[224] Work hardening due to this additional 8% plastic strain can account

for the ~200 MPa difference between the hardness and yield strength data, as shown by Brittain *et al.*[60] Such differences between hardness and yield strength measurements are seen in almost every metal's grain size strengthening data. The effect is most evident among studies on coarse-grained metals because they work harden to a greater extent than ultrafine grain or nanocrystalline metals.

In the supplementary material, we provide a summary of the experimental details from each of the Hall-Petch studies cited herein. This table includes the specimen purity, the processing techniques used to prepare the test specimens, the mechanical test method, and the technique used to measure the grain size. This information can be used to explain some of the differences in σ_0 among the various studies on a given metal.

Table 4: Interstitial content and corresponding solid solution strengthening increment in the Nb studies shown in Figure 7. The solid solution strengthening increments for oxygen and nitrogen are 0.19 and 0.41 MPa/ppm, respectively.[225]

	ppm by wt			
Ref.	O	N	$\sigma_{0,ss}$ (MPa)	σ_0 (MPa)
27	120	13	30	40
29	60	45	30	60
24	200	200	120	130
19	550	120	160	150
20	400	100	120	170
23	185	57	60	150

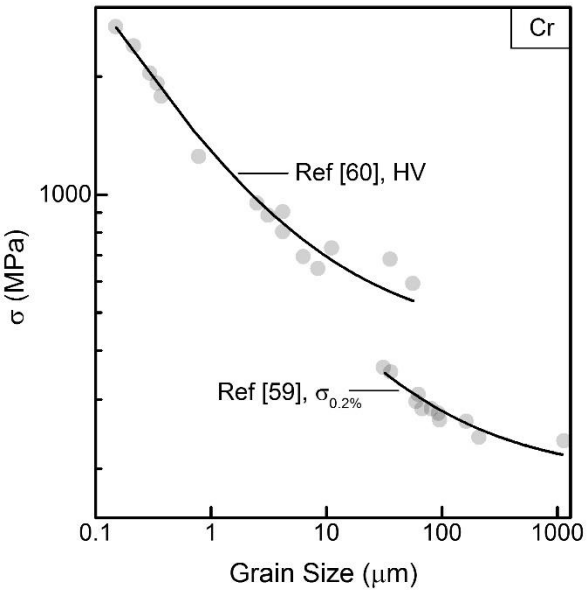

Figure 9: Chromium grain size strengthening data from Refs. 59, 60 as well as best fits using equation (1) to each study's data.

4. The Hall-Petch Breakdown

For coarse grained specimens, the preceding discussion demonstrates that the grain size strengthening increment can be estimated using equation (1) and the constants in Table 1, and that much of the variation among the different studies can be explained by some combination of specimen contamination and work hardening effects. However, data from a few of the datasets in Figures 1-3 (most notably that for Zn and Cu) illustrate that simply extrapolating the grain size strengthening behavior of coarse-grained samples to nanocrystalline grain sizes can result in errors: the strength measured in the finest grain size specimens can be less than that expected.[226, 227] This apparent breakdown of the Hall-Petch effect has been much discussed and debated, and it is clear that many of the observations of lowered strength levels in nanograined materials can be attributed to artefacts in sample processing. At the same time, it is physically reasonable that the Hall-Petch equation breaks down; for instance, if it did not, the yield strength of a tungsten specimen with a grain size of 10 nm would be larger than tungsten's theoretical yield strength, $G/15 = 10$ GPa.[228]

In-situ and ex-situ TEM investigations of plastic deformation in nanocrystalline nickel,[229, 230] copper,[231, 232] gold,[233] aluminium,[234] and platinum[235] show a transition in the dislocation behavior in very fine grained samples. These studies have shown that while there can be extensive dislocation activity in samples with grain sizes as small as 10 nm, dislocations do not accumulate in nanocrystalline metals as they do in coarse-grained samples. Instead, in nanocrystalline metals, dislocations emitted from one grain boundary are often rapidly absorbed by other grain boundaries after they traverse the grain interior. Measurements showing a plateau or even a decrease in the dislocation density at ~100 nm suggest that this transition in the dislocation behavior may also contribute to a lowering of the Hall-Petch slope at such grain sizes.[236, 237] In light of these results, it seems that the strength of nanocrystalline metals is determined by the stress required to nucleate, propagate, or reabsorb individual dislocations, and this motivated the dislocation-nucleation models of the Hall-Petch breakdown developed by Asaro and co-workers,[238-241] which are relevant in the range of grain sizes down to perhaps ~10 nm.

At the finest grain sizes there is considerable evidence that the Hall-Petch breakdown involves a weakening effect as grain size is reduced beyond about 10-20 nm. The effect is most thoroughly experimentally established on alloy systems in which such fine grains can be stabilized, and experimental data on pure metals with grain sizes in this range are rare and not usually systematic. It is the authors' opinion that conclusively demonstrating the Hall-Petch breakdown by experiments on a pure metal will be difficult or even impossible, because of the rapid grain growth in pure nanocrystalline metals at low homologous temperatures, the possibility of grain growth during plastic deformation, and the fact that grain boundary structure and state can affect strength to the same extent as grain size.[48] There are, however, several systematic computational studies on pure metals that convincingly demonstrate the inflection of strength at

a "strongest grain size."[242-245] The strength inflection at these fine grain sizes is associated with a transition to intergranular deformation mechanisms dominating flow. Ref. 246 argues that these mechanisms are very similar to those responsible for deformation in metallic glasses, and shows that many unusual metal properties emerge at the finest grain sizes that are consistent with such a picture: a loss of rate sensitivity in FCC metals, the emergence of pressure sensitivity, and a tendency for shear localization are three features of glass plasticity that support the Hall-Petch breakdown as being reflective of a cross-over to glass-like deformation physics in the intergranular regions.

Many of the other models that have been developed to explain the Hall-Petch breakdown are modified versions of those originally developed to explain equation (1). For example, one class of models, based on the pile-up concept, assume that the Hall-Petch breakdown occurs because either the grains in the nanocrystalline metals are too small to support a dislocation pile-up[179, 247, 248] or the grain size affects the pile-up's interactions with the grain boundaries.[249] There are also modified composite models in which the bulk material's strength is assumed to be the average of a weaker grain boundary phase and a stronger grain interior phase,[250-258] which is physically in line with the transition to intergranular "glass-like" plasticity described above. More detailed composite models account for additional microstructural features including triple junctions and quadruple nodes.[259-262] One hypothesized reason the grain boundaries appear weaker than the grain interior is that they accelerate Coble creep processes;[86, 260, 263, 264] however, because these Coble creep models require strain rate sensitivities that are inconsistent with measured values, their validity has been questioned.[265, 266]

5. Summary and Outlook

In this work, we calculated best estimates of the pure metals' Hall-Petch parameters using the grain size strengthening data accumulated over the past six decades. We also used these data to validate the Hall-Petch coefficient's dependence on crystal structure, the similarities between the frictional stress and single crystal flow stress, and several other trends. Some of these trends are accounted for in the dislocation pile-up model of grain size strengthening, but as we have noted, there is no direct evidence to support this model's underlying assumption that the grain size limits the size of dislocation pile-ups. Though the other explanations of grain-size strengthening that we summarized also have deficiencies, Ashby's geometrically necessary dislocation model appears to be the most consistent with the strain-dependence of the Hall-Petch coefficient and with experimental observations of the dislocation substructure in plastically deformed polycrystals with coarse grain sizes.

Our compilation of grain size strengthening measurements revealed several gaps in the open literature that should be addressed in future research. In addition to the obvious gaps related to, e.g., materials that have not yet been studied, there is a dearth of accurate strength measurements on samples with sub-micron grain

sizes, which is in part due to the difficulty of preparing bulk, defect-free, nanocrystalline specimens for standard tension and compression testing. Recently, many of these processing challenges have been overcome,[267, 268] and these advances in processing should enable more systematic investigations of grain size strengthening in ultrafine and nanocrystalline metals.

Future research on grain size strengthening should also address the relationship between grain size strengthening and grain boundary structure. This includes detailed work on grain boundary crystallography and the sampling of boundary crystallographic space in a polycrystal, as well as details associated with the thermodynamics of interface structure, i.e., grain boundary complexion.[269] While these topics have been actively studied in the grain boundary community for many years, the connection between boundary structure and grain size scaling behavior remains fertile territory for future work. Such connections would be especially relevant in materials with very fine grain sizes, where the grain boundaries themselves can accommodate plastic strain.

Insight into the relationship between grain boundary structure and strength may also come from studies on nanotwinned metals, which contain large populations of coherent twin boundaries with much smaller excess energies and free volumes than the high angle boundaries typically found in traditional nanocrystalline metals.[223] Because nanotwinned and traditional nanocrystalline metals have such disparate grain boundary structures, differences in their mechanical properties affected by grain boundary structure are maximized, and this makes such properties easier to identify. For example, initial studies comparing nanotwinned and nanocrystalline copper found that nanotwinned copper's yield strength exhibits a Hall-Petch type dependence on the mean twin spacing with a frictional stress and Hall-Petch coefficient similar to those of nanocrystalline copper, but that nanotwinned copper work-hardens faster than traditional nanocrystalline copper does.[270, 271] These results indicate that the effects of grain boundary structure on mechanical properties can persist to large plastic strains, which is an unexpected finding that should be further clarified.

Another topic that should be investigated in more detail is the grain size dependence of the yield stress of materials that mechanically twin. Several studies on BCC metals have shown that even when these materials twin, their yield stress is still related to the grain size through equation (1).[12, 59] These studies have also established that, at a given temperature, the Hall-Petch coefficient for twinning can be up to an order of magnitude greater than the Hall-Petch coefficient for dislocation glide.[272] Explanations of these behaviors have been proposed that are based on the dislocation pile-up concept[273] and the grain size dependence of the twin morphology,[274] but there is limited direct experimental validation of these theories. Future work on this topic will be of engineering value because it may help guide the design of microstructures that are more resistant to twinning and are therefore more ductile.

Though the Hall-Petch equation has been investigated for over half a century – and grain size strengthening for even longer – there are still many exciting and relatively unexplored avenues for future research. Work on these topics will benefit from recent developments in imaging, mechanical characterization, and processing, and any advances in understanding that are made through this work will have a significant impact on materials engineering, since they will enable ever finer control over the mechanical properties of metals.

Acknowledgements—The authors acknowledge the partial support of several agencies in the development of this review, including the U.S. Army Research Office under grant W911NF-14-1-0539 and through the Institute for Soldier Nanotechnologies at MIT, as well as the U.S. National Science Foundation under grant CMMI-1332789.

References

1. E. O. Hall: 'The deformation and ageing of mild steel: III discussion of results', *Proc. Phys. Soc., Sect. B*, 1951, **64**(9), 747-755.
2. N. J. Petch: 'The cleavage strength of polycrystals', *J. Iron Steel Inst.*, 1953, **174**(1), 25-28.
3. R. W. Armstrong: 'The influence of polycrystal grain size on several mechanical properties of materials', *Metall. Mater. Trans.*, 1970, **1**(5), 1169-1176.
4. N. Hansen: 'Polycrystalline strengthening', *Metall. Trans. A*, 1985, **16**(12), 2167-2190.
5. A. Lasalmonie and J. L. Strudel: 'Influence of grain size on the mechanical behaviour of some high strength materials', *J. Mater. Sci.*, 1986, **21**(6), 1837-1852.
6. E. D. Levine, J. P. Pemsler, and S. H. Gelles: 'Characteristics of vacuum-distilled beryllium', *J. Nucl. Mater.*, 1964, **12**(1), 40-49.
7. F. E. Hauser, P. R. Landon, and J. E. Dorn: 'Fracture of magnesium alloys at low temperature', *Trans. Am. Inst. Metall. Eng.*, 1956, **48**(5), 589-593.
8. F. Hultgren: 'Grain boundary and substructure hardening in aluminum', *Trans. Am. Inst. Metall. Eng.*, 1964, **230**(4), 898-903.
9. J. C. M. Li and Y. T. Chou: 'The role of dislocations in the flow stress grain size relationships', *Metall. Mater. Trans.*, 1970, **1**(5), 1145-1159.
10. G. S. Rao and Y. V. R. K. Prasad: 'Grain boundary strengthening in strongly textured magnesium produced by hot rolling', *Metall. Trans. A*, 1982, **13**(12), 2219-2226.
11. Y. Wang and H. Choo: 'Influence of texture on Hall–Petch relationships in an Mg alloy', *Acta Mater.*, 2014, **81**, 83-97.
12. T. G. Lindley and R. E. Smallman: 'The plastic deformation of polycrystalline vanadium at low temperatures', *Acta Metall.*, 1963, **11**(5), 361-371.
13. M. A. Sherman and R. F. Bunshah: 'Yield strength of fine-grained vanadium produced by high-rate physical vapor deposition', *J. Nucl. Mater.*, 1975, **57**(2), 151-154.
14. A. F. Jankowski, J. Go, and J. P. Hayes: 'Thermal stability and mechanical behavior of ultra-fine bcc Ta and V coatings', *Surf. Coat. Tech.*, 2007, **202**(4), 957-961.
15. Y. B. Chun, S. H. Ahn, D. H. Shin, and S. K. Hwang: 'Combined effects of grain size and recrystallization on the tensile properties of cryorolled pure vanadium', *Mater. Sci. Eng.: A*, 2009, **508**(1), 253-258.
16. G. Nouet and A. Deschanvres: 'Relations entre les essais de dureté et de traction et la taille des grains dans le vanadium', *J. Less Common Met.*, 1974, **35**(1), 17-29.
17. D. H. Sherman, C. V. Owen, and T. E. Scott: 'The effect of hydrogen on the structure and properties of vanadium', *Trans. Am. Inst. Metall. Eng.*, 1969, **245**(6), 1367-1369.
18. Q. Wei, T. Jiao, K. T. Ramesh, and E. Ma: 'Nano-structured vanadium: processing and mechanical properties under quasi-static and dynamic compression', *Scripta Mater.*, 2004, **50**(3), 359-364.
19. Z. C. Szkopiak: 'The Hall-Petch parameters of niobium determined by the grain size and extrapolation methods', *Mater. Sci. Eng.*, 1972, **9**(1), 7-13.
20. A. T. Churchman: 'Cleavage fracture in niobium', *J. Inst. Met.*, 1960, **88**, 221-222.
21. E. N. Popova, V. V. Popov, E. P. Romanov, and V. P. Pilyugin: 'Effect of the degree of deformation on the structure and thermal stability of nanocrystalline niobium produced by high-pressure torsion', *Phys. Met. Metall.*, 2007, **103**(4), 407-413.
22. E. N. Popova, V. V. Popov, E. P. Romanov, and V. P. Pilyugin: 'Thermal stability of nanocrystalline Nb produced by severe plastic deformation', *Phys. Met. Metall.*, 2006, **101**(1), 52-57.
23. P. R. V. Evans, A. F. Weinberg, and R. J. Van Thyne: 'Irradiation hardening in columbium', *Acta Metall.*, 1963, **11**(2), 143-150.
24. B. A. Wilcox and R. A. Huggins: 'Effect of hydrogen on dislocation locking in niobium', *J. Less Common Met.*, 1960, **2**(2), 292-303.

25. M. A. Adams, A. C. Roberts, and R. E. Smallman: 'Yield and fracture in polycrystalline niobium', *Acta Metall.*, 1960, **8**(5), 328-337.
26. A. A. Johnson: 'The low temperature tensile properties of niobium', *Acta Metall.*, 1960, **8**(10), 737-740.
27. A. M. Omar and A. R. Entwisle: 'The effect of grain size on the deformation of niobium', *Mater. Sci. Eng.*, 1970, **5**(5), 263-270.
28. V. V. Popov, E. N. Popova, A. V. Stolbovskii, V. P. Pilyugin, and N. K. Arkhipova: 'Nanostructurization of Nb by high-pressure torsion in liquid nitrogen and the thermal stability of the structure obtained', *Phys. Met. Metall.*, 2012, **113**(3), 295-301.
29. H. Conrad, S. Feuerstein, and L. Rice: 'Effects of grain size on the dislocation density and flow stress of niobium', *Mater. Sci. Eng.*, 1967, **2**(3), 157-168.
30. A. F. Jankowski, J. P. Hayes, and C. K. Saw: 'Dimensional attributes in enhanced hardness of nanocrystalline Ta–V nanolaminates', *Philos. Mag.*, 2007, **87**(16), 2323-2334.
31. R. C. Koo: 'Grain-size effects on the deformation of tantalum at low temperatures', *J. Less Common Met.*, 1962, **4**(2), 138-144.
32. M. A. Adams and A. Iannucci, *The mechanical properties of tantalum with special reference to the ductile-brittle transition*, M. R. Corp, Editor. 1961: Yonkers, NY.
33. K. T. Hartwig, S. N. Mathaudhu, H. J. Maier, and I. Karaman: 'Hardness and microstructure changes in severely deformed and recrystallized tantalum', 2nd Int. Symp. on Ultrafine Grained Materials, Seattle, WA, 2002, 151-160.
34. S. N. Mathaudhu and K. T. Hartwig: 'Grain refinement and recrystallization of heavily worked tantalum', *Mater. Sci. Eng.: A*, 2006, **426**(1), 128-142.
35. M. Zhang, B. Yang, J. Chu, and T. G. Nieh: 'Hardness enhancement in nanocrystalline tantalum thin films', *Scripta Mater.*, 2006, **54**(7), 1227-1230.
36. H. L. Sun and M. Wei: 'Microstructure and nanoindentation hardness of sputter deposited nanocrystalline tantalum thin films', Adv. Mater. Res., 2011, Trans Tech Publ, 1810-1813.
37. G. Guisbiers, E. Herth, L. Buchaillot, and T. Pardoen: 'Fracture toughness, hardness, and Young's modulus of tantalum nanocrystalline films', *Appl. Phys. Let.*, 2010, **97**(14), 143115.
38. D. J. Dingley and D. McLean: 'Components of the flow stress of iron', *Acta Metall.*, 1967, **15**(5), 885-901.
39. R. A. Jago and N. Hansen: 'Grain size effects in the deformation of polycrystalline iron', *Acta Metall.*, 1986, **34**(9), 1711-1720.
40. H. H. Tjerkstra: 'The effect of grain size on the stress-strain curve of alpha-iron and the connection with the plastic deformation of the grain boundaries', *Acta Metall.*, 1961, **9**(4), 259-263.
41. I. Codd and N. J. Petch: 'Dislocation-locking by carbon, nitrogen and boron in α-iron', *Philos. Mag.*, 1960, **5**(49), 30-42.
42. A. Cracknell and N. J. Petch: 'Frictional forces on dislocation arrays at the lower yield point in iron', *Acta Metall.*, 1955, **3**(2), 186-189.
43. J. Heslop and N. J. Petch: 'The stress to move a free dislocation in alpha iron', *Philos. Mag.*, 1956, **47**(9), 866-873.
44. N. J. Petch: 'The ductile-brittle transition in the fracture of α-iron: I', *Philos. Mag.*, 1958, **3**(34), 1089-1097.
45. H. Conrad and G. Schoeck: 'Cottrell locking and the flow stress in iron', *Acta Metall.*, 1960, **8**(11), 791-796.
46. J. S. C. Jang and C. C. Koch: 'The Hall-Petch relationship in nanocrystalline iron produced by ball milling', *Scripta Metall. Mater.*, 1990, **24**(8), 1599-1604.
47. T. R. Malow and C. C. Koch: 'Mechanical properties, ductility, and grain size of nanocrystalline iron produced by mechanical attrition', *Metall. Mater. Trans. A*, 1998, **29**(9), 2285-2295.
48. D. Jang and M. Atzmon: 'Grain-size dependence of plastic deformation in nanocrystalline Fe', *J. Appl. Phys.*, 2003, **93**(11), 9282-9286.

49. M. M. Hutchison: 'The temperature dependence of the yield stress of polycrystalline iron', *Philos. Mag.*, 1963, **8**(85), 121-127.
50. E. Anderson, D. Law, W. King, and J. Spreadborough: 'The relationship between lower yield stress and grain size in Armco iron', *Trans. Am. Inst. Metall. Eng.*, 1968, **242**(1), 115-119.
51. J. F. Butler: 'Lüders front propagation in low carbon steels', *J. Mech. Phys. Sol.*, 1962, **10**(4), 313-318.
52. D. Hull and I. L. Mogford: 'Ductile-brittle transition in steels irradiated with neutrons', *Philos. Mag.*, 1958, **3**(35), 1213-1222.
53. T. D. Shen, R. B. Schwarz, S. Feng, J. G. Swadener, J. Y. Huang, M. Tang, J. Zhang, S. C. Vogel, and Y. Zhao: 'Effect of solute segregation on the strength of nanocrystalline alloys: Inverse Hall–Petch relation', *Acta Mater.*, 2007, **55**(15), 5007-5013.
54. J. B. Savader, M. R. Scanlon, R. C. Cammarata, D. T. Smith, and C. Hayzelden: 'Nanoindentation study of sputtered nanocrystalline iron thin films', *Scripta Mater.*, 1997, **36**(1), 29-34.
55. W. B. Morrison: 'The effect of grain size on the stress-strain relationship in low-carbon steel', *Trans. Am. Soc. Metall.*, 1966, **59**(4), 824-846.
56. S. Gao, M. Chen, M. Joshi, A. Shibata, and N. Tsuji: 'Yielding behavior and its effect on uniform elongation in IF steel with various grain sizes', *J. Mater. Sci.*, 2014, **49**(19), 6536-6542.
57. V. Provenzano, R. Valiev, D. G. Rickerby, and G. Valdre: 'Mechanical properties of nanostructured chromium', *Nanostruc. Mater.*, 1999, **12**(5), 1103-1108.
58. D. Wu, J. Zhang, J. C. Huang, H. Bei, and T. Nieh: 'Grain-boundary strengthening in nanocrystalline chromium and the Hall–Petch coefficient of body-centered cubic metals', *Scripta Mater.*, 2013, **68**(2), 118-121.
59. M. J. Marcinkowski and H. A. Lipsitt: 'The plastic deformation of chromium at low temperatures', *Acta Metall.*, 1962, **10**(2), 95-111.
60. C. P. Brittain, R. W. Armstrong, and G. C. Smith: 'Hall-petch dependence for ultrafine grain size electrodeposited chromium', *Scripta Metall.*, 1985, **19**(1), 89-91.
61. A. A. Johnson: 'The effect of grain size on the tensile properties of high-purity molybdenum at room temperature', *Philos. Mag.*, 1959, **4**(38), 194-199.
62. A. S. Wronski and A. A. Johnson: 'The deformation and fracture properties of polycrystalline molybdenum', *Philos. Mag.*, 1962, **7**(74), 213-227.
63. M. A. Sherman, R. F. Bunshah, and H. A. Beale: 'High-rate physical vapor deposition of refractory metals', *J. Vac. Sci. Tech.*, 1975, **12**(3), 697-703.
64. C. M. McNally, W. H. Kao, and T. G. Nieh: 'The effect of potassium doping on the strength of molybdenum', *Scripta Metall.*, 1988, **22**(12), 1847-1850.
65. K. B. Yoder, A. A. El-Mustafa, J. C. Lin, R. A. Hoffman, and D. S. Stone: 'Activation analysis of deformation in evaporated molybdenum thin films', *J. Phys. D: Appl. Phys.*, 2003, **36**(7), 884.
66. A. G. Imgram, J. W. Spretnak, and H. R. Ogden: 'Effect of metallurgical structure on the tensile and notch-tensile properties of molybdenum and Mo-0.5Ti', *Trans. Am. Inst. Metall. Eng.*, 1964, **230**, 1345-1352.
67. E. S. Meieran and D. A. Thomas: 'Structure of drawn and annealed tungsten wire', *Trans. Am. Inst. Metall. Eng.*, 1965, **233**, 937-943.
68. U. K. Vashi, R. W. Armstrong, and G. E. Zima: 'The hardness and grain size of consolidated fine tungsten powder', *Metall. Trans.*, 1970, **1**(6), 1769-1771.
69. A. W. Thompson and W. A. Backofen: 'Production and mechanical behavior of very fine-grained copper', *Metall. Trans.*, 1971, **2**(7), 2004-2005.
70. N. Ono and S. Karashima: 'Grain size dependence of flow stress in copper polycrystals', *Scripta Metall.*, 1982, **16**(4), 381-384.
71. N. Hansen and B. Ralph: 'The strain and grain size dependence of the flow stress of copper', *Acta Metall.*, 1982, **30**(2), 411-417.
72. P. Feltham and J. D. Meakin: 'On the mechanism of work hardening in face-centred cubic metals, with special reference to polycrystalline copper', *Philos. Mag.*, 1957, **2**(13), 105-112.

73. M. D. Merz and S. D. Dahlgren: 'Tensile strength and work hardening of ultrafine-grained high-purity copper', *J. Appl. Phys.*, 1975, **46**(8), 3235-3237.
74. P. G. Sanders, J. A. Eastman, and J. R. Weertman: 'Elastic and tensile behavior of nanocrystalline copper and palladium', *Acta Mater.*, 1997, **45**(10), 4019-4025.
75. C. J. Youngdahl, P. G. Sanders, J. A. Eastman, and J. R. Weertman: 'Compressive yield strengths of nanocrystalline Cu and Pd', *Scripta Mater.*, 1997, **37**(6), 809-813.
76. J. Chen, L. Lu, and K. Lu: 'Hardness and strain rate sensitivity of nanocrystalline Cu', *Scripta Mater.*, 2006, **54**(11), 1913-1918.
77. A. S. Khan, B. Farrokh, and L. Takacs: 'Compressive properties of Cu with different grain sizes: sub-micron to nanometer realm', *J. Mater. Sci.*, 2008, **43**(9), 3305-3313.
78. R. P. Carreker and W. R. Hibbard: 'Tensile deformation of high-purity copper as a function of temperature, strain rate, and grain size', *Acta Metall.*, 1953, **1**(6), 654-663.
79. G. W. Nieman, J. R. Weertman, and R. W. Siegel: 'Mechanical behavior of nanocrystalline Cu and Pd', *J. Mater. Res.*, 1991, **6**(5), 1012-1027.
80. G. E. Fougere, J. R. Weertman, R. W. Siegel, and S. Kim: 'Grain-size dependent hardening and softening of nanocrystalline Cu and Pd', *Scripta Metall. Mater.*, 1992, **26**(12), 1879-1883.
81. V. Y. Gertsman, M. Hoffmann, H. Gleiter, and R. Birringer: 'The study of grain size dependence of yield stress of copper for a wide grain size range', *Acta Metall. Mater.*, 1994, **42**(10), 3539-3544.
82. M. Hakamada, Y. Nakamoto, H. Matsumoto, H. Iwasaki, Y. Chen, H. Kusuda, and M. Mabuchi: 'Relationship between hardness and grain size in electrodeposited copper films', *Mater. Sci. Eng.: A*, 2007, **457**(1), 120-126.
83. R. Suryanarayanan, C. A. Frey, S. M. L. Sastry, B. E. Waller, S. E. Bates, and W. E. Buhro: 'Mechanical properties of nanocrystalline copper produced by solution-phase synthesis', *J. Mater. Res.*, 1996, **11**(2), 439-448.
84. H. Jiang, Y. T. Zhu, D. P. Butt, I. V. Alexandrov, and T. C. Lowe: 'Microstructural evolution, microhardness and thermal stability of HPT-processed Cu', *Mater. Sci. Eng.: A*, 2000, **290**(1), 128-138.
85. A. W. Thompson and M. I. Baskes: 'The influence of grain size on the work hardening of face-center cubic polycrystals', *Philos. Mag.*, 1973, **28**(2), 301-308.
86. A. H. Chokshi, A. Rosen, J. Karch, and H. Gleiter: 'On the validity of the Hall-Petch relationship in nanocrystalline materials', *Scripta Metall.*, 1989, **23**(10), 1679-1683.
87. J. W. Aldrich and R. W. Armstrong: 'The grain size dependence of the yield, flow and fracture stress of commercial purity silver', *Metall. Trans.*, 1970, **1**(9), 2547-2550.
88. N. P. Kobelev, Y. M. Soifer, R. A. Andrievski, and B. Gunther: 'Microhardness and elastic properties of nanocrystalline silver', *Nanostruc. Mater.*, 1993, **2**(5), 537-544.
89. X. Y. Qin, X. J. Wu, and L. D. Zhang: 'The microhardness of nanocrystalline silver', *Nanostruc. Mater.*, 1995, **5**(1), 101-110.
90. R. P. Carreker: 'Tensile deformation of silver as a function of temperature, strain rate, and grain size', *Trans. Am. Inst. Metall. Eng.*, 1957, **209**, 112-115.
91. T. Kizuka, H. Ichinose, and Y. Ishida: 'Structure and hardness of nanocrystalline silver', *J. Mater. Sci.*, 1997, **32**(6), 1501-1507.
92. C. C. Lo, J. A. Augis, and M. R. Pinnel: 'Hardening mechanisms of hard gold', *J. Appl. Phys.*, 1979, **50**(11), 6887-6891.
93. S. Sakai, H. Tanimoto, and H. Mizubayashi: 'Mechanical behavior of high-density nanocrystalline gold prepared by gas deposition method', *Acta Mater.*, 1998, **47**(1), 211-217.
94. R. D. Emery and G. L. Povirk: 'Tensile behavior of free-standing gold films. Part II. Fine-grained films', *Acta Mater.*, 2003, **51**(7), 2079-2087.
95. Y. M. Wang, A. F. Jankowski, and A. V. Hamza: 'Strength and thermal stability of nanocrystalline gold alloys', *Scripta Mater.*, 2007, **57**(4), 301-304.

96. S. Floreen and J. H. Westbrook: 'Grain boundary segregation and the grain size dependence of strength of nickel-sulfur alloys', *Acta Metall.*, 1969, **17**(9), 1175-1181.
97. D. E. Sonon and G. V. Smith: 'Effect of grain size and temperature on the strengthening of nickel and a nickel-cobalt alloy by carbon', *Trans. Am. Inst. Metall. Eng.*, 1968, **242**(8), 1527-1533.
98. Y. Nakada and A. S. Keh: 'Solid-solution strengthening in Ni-C alloys', *Metall. Trans.*, 1971, **2**(2), 441-447.
99. B. A. Wilcox and A. H. Clauer: 'The role of grain size and shape in strengthening of dispersion hardened nickel alloys', *Acta Metall.*, 1972, **20**(5), 743-757.
100. A. W. Thompson: 'Yielding in nickel as a function of grain or cell size', *Acta Metall.*, 1975, **23**(11), 1337-1342.
101. G. D. Hughes, S. D. Smith, C. S. Pande, H. R. Johnson, and R. W. Armstrong: 'Hall-Petch strengthening for the microhardness of twelve nanometer grain diameter electrodeposited nickel', *Scripta Metall.*, 1986, **20**(1), 93-97.
102. A. M. El-Sherik, U. Erb, G. Palumbo, and K. T. Aust: 'Deviations from Hall-Petch behaviour in as-prepared nanocrystalline nickel', *Scripta Metall. Mater.*, 1992, **27**(9), 1185-1188.
103. F. Ebrahimi, G. R. Bourne, M. S. Kelly, and T. E. Matthews: 'Mechanical properties of nanocrystalline nickel produced by electrodeposition', *Nanostruc. Mater.*, 1999, **11**(3), 343-350.
104. M. von Heimendahl and G. Thomas: 'Substructure and mechanical properties of TD-nickel', *Trans. Am. Inst. Metall. Eng.*, 1964, **230**(7), 1520-1528.
105. A. Godon, J. Creus, S. Cohendoz, E. Conforto, X. Feaugas, P. Girault, and C. Savall: 'Effects of grain orientation on the Hall–Petch relationship in electrodeposited nickel with nanocrystalline grains', *Scripta Mater.*, 2010, **62**(6), 403-406.
106. C. A. Schuh, T. G. Nieh, and T. Yamasaki: 'Hall–Petch breakdown manifested in abrasive wear resistance of nanocrystalline nickel', *Scripta Mater.*, 2002, **46**(10), 735-740.
107. J. A. Knapp and D. M. Follstaedt: 'Hall–Petch relationship in pulsed-laser deposited nickel films', *J. Mater. Res.*, 2004, **19**(1), 218-227.
108. N. Hansen: 'The effect of grain size and strain on the tensile flow stress of aluminium at room temperature', *Acta Metall.*, 1977, **25**(8), 863-869.
109. H. Fujita and T. Tabata: 'The effect of grain size and deformation sub-structure on mechanical properties of polycrystalline aluminum', *Acta Metall.*, 1973, **21**(4), 355-365.
110. N. Hansen: 'Effect of grain size on the mechanical properties of dipersion-strengthened aluminium aluminium-oxide products', *Trans. Am. Inst. Metall. Eng.*, 1969, **245**(6), 1305-1312.
111. J. W. Wyrzykowski and M. W. Grabski: 'Effect of annealing temperature on structure and properties of fine-grained aluminium', *Met. Sci.*, 1983, **17**(9), 445-450.
112. J. T. Al-Haidary, N. J. Petch, and E. R. De Los Rios: 'The plastic deformation of polycrystals I. Aluminium between room temperature and 400° C', *Philos. Mag. A*, 1983, **47**(6), 869-890.
113. E. Bonetti, L. Pasquini, and E. Sampaolesi: 'The influence of grain size on the mechanical properties of nanocrystalline aluminium', *Nanostruc. Mater.*, 1997, **9**(1), 611-614.
114. N. Tsuji, Y. Ito, Y. Saito, and Y. Minamino: 'Strength and ductility of ultrafine grained aluminum and iron produced by ARB and annealing', *Scripta Mater.*, 2002, **47**(12), 893-899.
115. Y. S. Sato, M. Urata, H. Kokawa, and K. Ikeda: 'Hall–Petch relationship in friction stir welds of equal channel angular-pressed aluminium alloys', *Mater. Sci. Eng.: A*, 2003, **354**(1), 298-305.
116. R. W. Hayes, D. Witkin, F. Zhou, and E. Lavernia: 'Deformation and activation volumes of cryomilled ultrafine-grained aluminum', *Acta Mater.*, 2004, **52**(14), 4259-4271.
117. C. Y. Yu, P. W. Kao, and C. P. Chang: 'Transition of tensile deformation behaviors in ultrafine-grained aluminum', *Acta Mater.*, 2005, **53**(15), 4019-4028.
118. A. S. Khan, B. Farrokh, and L. Takacs: 'Effect of grain refinement on mechanical properties of ball-milled bulk aluminum', *Mater. Sci. Eng.: A*, 2008, **489**(1), 77-84.
119. A. S. Khan, Y. S. Suh, X. Chen, L. Takacs, and H. Zhang: 'Nanocrystalline aluminum and iron: mechanical behavior at quasi-static and high strain rates, and constitutive modeling', *Int. J. Plast.*, 2006, **22**(2), 195-209.

120. K. Maung, J. C. Earthman, and F. A. Mohamed: 'Inverse Hall–Petch behavior in diamantane stabilized bulk nanocrystalline aluminum', *Acta Mater.*, 2012, **60**(16), 5850-5857.
121. R. Carreker and W. Hibbard: 'Tensile deformation of aluminum as a function of temperature, strain rate, and grain size', *Trans. Am. Inst. Metall. Eng.*, 1957, **209**, 1157-1163.
122. P. L. Sun, E. K. Cerreta, G. T. Gray III, and J. F. Bingert: 'The effect of grain size, strain rate, and temperature on the mechanical behavior of commercial purity aluminum', *Metall. Mater. Trans. A*, 2006, **37**(10), 2983-2994.
123. R. L. Jones and H. Conrad: 'The effect of grain size on the strength of alpha-titanium at room temperature', *Trans. Am. Inst. Metall. Eng.*, 1969, **245**(4), 779-789.
124. R. J. Lederich, S. M. L. Sastry, J. E. O'Neal, and B. B. Rath: 'The effect of grain size on yield stress and work hardening of polycrystalline titanium at 295 K and 575 K', *Mater. Sci. Eng.*, 1978, **33**(2), 183-188.
125. K. Y. Wang, T. D. Shen, M. X. Quan, and W. D. Wei: 'Hall-Petch relationship in nanocrystalline titanium produced by ball-milling', *J. Mater. Sci. Let.*, 1993, **12**(23), 1818-1820.
126. A. A. Popov, I. Y. Pyshmintsev, S. L. Demakov, A. G. Illarionov, T. C. Lowe, A. V. Sergeyeva, and R. Z. Valiev: 'Structural and mechanical properties of nanocrystalleve titanium processed by severe plastic deformation', *Scripta Mater.*, 1997, **37**(7), 1089-1094.
127. A. V. Sergueeva, V. V. Stolyarov, R. Z. Valiev, and A. K. Mukherjee: 'Advanced mechanical properties of pure titanium with ultrafine grained structure', *Scripta Mater.*, 2001, **45**(7), 747-752.
128. C. Y. Hyun, J. H. Lee, and H. K. Kim: 'Microstructures and mechanical properties of ultrafine grained pure Ti produced by severe plastic deformation', *Res. Chem. Intermediates*, 2010, **36**(6), 629-638.
129. A. Ghaderi and M. R. Barnett: 'Sensitivity of deformation twinning to grain size in titanium and magnesium', *Acta Mater.*, 2011, **59**(20), 7824-7839.
130. F. C. Holden, H. R. Ogden, and R. I. Jaffee: 'Microstructure and mechanical properties of iodide titanium', *Trans. Am. Inst. Metall. Eng.*, 1953, **197**(2), 238-242.
131. K. Okazaki and H. Conrad: 'Effects of interstitial content and grain size on the strength of titanium at low temperatures', *Acta Metall.*, 1973, **21**(8), 1117-1129.
132. H. Hu and R. S. Cline: 'Mechanism of reorientation during recrystallization of polycrystalline titanium', *Trans. Met. Soc. AIME*, 1968, **242**(6).
133. C. E. Coleman and D. Hardie: 'Grain-size dependence in the flow and fracture of alpha zirconium', *J. Inst. Met.*, 1966, **94**(11), 387-391.
134. S. V. Ramani and P. Rodriguez: 'Grain size dependence of the deformation behaviour of alpha zirconium', *Can. Metall. Q.*, 1972, **11**(1), 61-67.
135. D. J. Abson and J. J. Jonas: 'Substructure strengthening in zirconium and zirconium-tin alloys', *J. Nucl. Mater.*, 1972, **42**(1), 73-85.
136. C. Yuan, R. Fu, F. Zhang, X. Zhang, and F. Liu: 'Microstructure evolution and mechanical properties of nanocrystalline zirconium processed by surface circulation rolling treatment', *Mater. Sci. Eng.: A*, 2013, **565**, 27-32.
137. L. Jiang, M. T. Pérez-Prado, P. A. Gruber, E. Arzt, O. A. Ruano, and M. E. Kassner: 'Texture, microstructure and mechanical properties of equiaxed ultrafine-grained Zr fabricated by accumulative roll bonding', *Acta Materialia*, 2008, **56**(6), 1228-1242.
138. E. K. Cerreta, C. A. Yablinsky, G. T. Gray, S. C. Vogel, and D. W. Brown: 'The influence of grain size and texture on the mechanical response of high purity hafnium', *Mater. Sci. Eng.: A*, 2007, **456**(1), 243-251.
139. A. A. Karimpoor and U. Erb: 'Mechanical properties of nanocrystalline cobalt', *Phys. Stat. Sol. (a)*, 2006, **203**(6), 1265-1270.
140. A. A. Karimpoor, K. T. Aust, and U. Erb: 'Charpy impact energy of nanocrystalline and polycrystalline cobalt', *Scripta Mater.*, 2007, **56**(3), 201-204.
141. A. A. Karimpoor, U. Erb, K. T. Aust, and G. Palumbo: 'High strength nanocrystalline cobalt with high tensile ductility', *Scripta Mater.*, 2003, **49**(7), 651-656.

142. Y. M. Wang, R. T. Ott, T. Van Buuren, T. M. Willey, M. M. Biener, and A. V. Hamza: 'Controlling factors in tensile deformation of nanocrystalline cobalt and nickel', *Phys. Rev. B*, 2012, **85**(1), 14101.
143. J. Sort, A. Zhilyaev, M. Zielinska, J. Nogués, S. Surinach, J. Thibault, and M. D. Baró: 'Microstructural effects and large microhardness in cobalt processed by high pressure torsion consolidation of ball milled powders', *Acta Mater.*, 2003, **51**(20), 6385-6393.
144. K. Hayashi and H. Etoh: 'Pressure sintering of iron, cobalt, nickel and copper ultrafine powders and the crystal grain size and hardness of the compacts', *Mater. Trans., JIM*, 1989, **30**(11), 925-931.
145. S. Gelles, V. Nerses, and J. Siergie: 'Beryllium as a structural material: How great a deterrent is its lack of ductility?', *J. Met.*, 1963, **15**, 843-848.
146. D. Webster, R. L. Greene, and R. W. Lawley: 'Factors controlling the strength and ductility of high purity beryllium block', *Metall. Trans.*, 1974, **5**(1), 91-96.
147. I. N. Khristenko, I. I. Papirov, and G. F. Tikhinskii: 'Effect of structural factors on the yield strength of beryllium', *Met. Sci. & Heat Treatment*, 1976, **18**(7), 597-600.
148. B. C. Odegard Jr: 'Influence of purity level on the mechanical properties of hot isostatically pressed beryllium', Sandia Laboratory, 1979.
149. B. K. Kardashev and I. B. Kupriyanov: 'Elastic, micro- and macroplastic properties of polycrystalline beryllium', *Physics of the Solid State*, 2011, **53**(12), 2480-2485.
150. G. J. London, G. H. Keith, and N. P. Pinto: 'Grain size and oxide content affect beryllium's properties', *Met. Eng. Q.*, 1976, **16**(4), 45-57.
151. V. E. Ivanov, G. F. Tikhinskij, I. I. Papirov, I. A. Taranenko, and L. A. Kornienko: 'Grain size effect on mechanical properties of beryllium', *Phys. Met. Metall.*, 1979, **47**(2), 420-424.
152. B. Allen and A. Moore: 'The tough-brittle transition in beryllium', Conf. on the Metall. of Beryllium, London, 1961.
153. M. Kawasaki, S. Sato, T. Oku, K. Kida, and S. Nishigaki: 'Studies on the mechanical properties of Japanese beryllium', Conf. Int. Metallurgie Beryllium, Univ. de France, Paris, 1965.
154. F. Aldinger, E. Gold, and G. Petzow: 'Effects of oxide and grain size in high-purity beryllium', Fourth Int. Conf. on Beryllium, London, UK, 1977.
155. A. F. Jankowski, M. A. Wall, A. W. Van Buuren, T. G. Nieh, and J. Wadsworth: 'From nanocrystalline to amorphous structure in beryllium-based coatings', *Acta Mater.*, 2002, **50**(19), 4791-4800.
156. G. I. Turner and R. A. Lane: 'The effect of powder particle size on the mechanical properties of hot pressed high purity beryllium', Fourth Int. Conf. on Beryllium, London, UK, 1977.
157. D. V. Wilson and J. A. Chapman: 'Effects of preferred orientation on the grain size dependence of yield strength in metals', *Philos. Mag.*, 1963, **8**(93), 1543-1551.
158. D. V. Wilson: 'Ductility of polycrystalline magensium below 300 K', *J. Inst. Met.*, 1970, **98**(5), 133-143.
159. N. Ono, R. Nowak, and S. Miura: 'Effect of deformation temperature on Hall–Petch relationship registered for polycrystalline magnesium', *Mater. Let.*, 2004, **58**(1), 39-43.
160. H. J. Choi, Y. Kim, J. H. Shin, and D. H. Bae: 'Deformation behavior of magnesium in the grain size spectrum from nano-to micrometer', *Mater. Sci. Eng.: A*, 2010, **527**(6), 1565-1570.
161. J. Li, W. Xu, X. Wu, H. Ding, and K. Xia: 'Effects of grain size on compressive behaviour in ultrafine grained pure Mg processed by equal channel angular pressing at room temperature', *Mater. Sci. Eng.: A*, 2011, **528**(18), 5993-5998.
162. C. H. Caceres, G. E. Mann, and J. R. Griffiths: 'Grain size hardening in Mg and Mg-Zn solid solutions', *Metall. Mater. Trans. A*, 2011, **42**(7), 1950-1959.
163. J. A. Sharon, Y. Zhang, F. Mompiou, M. Legros, and K. J. Hemker: 'Discerning size effect strengthening in ultrafine-grained Mg thin films', *Scripta Mater.*, 2014, **75**, 10-13.
164. R. W. Armstrong, I. Codd, R. M. Douthwaite, and N. J. Petch: 'The plastic deformation of polycrystalline aggregates', *Philos. Mag.*, 1962, **7**(73), 45-58.

165. F. Chmelik, Z. Trojanova, P. Lukáč, and Z. Převorovský: 'Acoustic emission from zinc deformed at room temperature Part II The influence of grain size on deformation behaviour and acoustic emission of pure zinc', *J. Mater. Sci. Let.*, 1993, **12**(15), 1166-1168.
166. X. Zhang, H. Wang, R. O. Scattergood, J. Narayan, and C. C. Koch: 'Evolution of microstructure and mechanical properties of in situ consolidated bulk ultra-fine-grained and nanocrystalline Zn prepared by ball milling', *Mater. Sci. Eng.: A*, 2003, **344**(1), 175-181.
167. X. K. Zhu, X. Zhang, H. Wang, A. V. Sergueeva, A. K. Mukherjee, R. O. Scattergood, J. Narayan, and C. C. Koch: 'Synthesis of bulk nanostructured Zn by combinations of cryomilling and powder consolidation by room temperature milling: optimizing mechanical properties', *Scripta Mater.*, 2003, **49**(5), 429-433.
168. H. Mueller and F. Haessner: 'Influence of grain size and texture on the flow stress of zinc', *Scripta Metall.*, 1981, **15**(5), 487-492.
169. H. Conrad and J. Narayan: 'Mechanisms for grain size hardening and softening in Zn', *Acta Mater.*, 2002, **50**(20), 5067-5078.
170. J. Narayan, R. K. Venkatesan, and A. Kvit: 'Structure and properties of nanocrystalline zinc films', *J. Nanoparticle Res.*, 2002, **4**(3), 265-269.
171. P. Dusek and P. Lukac: 'Deformation of zinc polycrystals at room temperature', *Kovove Materialy*, 1979, **17**(5), 538-545.
172. N. R. Risebrough and E. Teghtsoonian: 'The linear hardening of cadmium', *Can. J. Phys.*, 1967, **45**(2), 591-605.
173. S. L. Mannan and P. Rodriguez: 'Grain size dependence of the deformation behaviour of cadmium', *Acta Metall.*, 1975, **23**(2), 221-228.
174. W. J. M. Tegart: 'Tensile properties of polycrystalline cadmium and some cadmium alloys in the range -196 to 200 °C', *J. Inst. Met.*, 1962, **91**(3), 99-104.
175. P. G. Sanders, C. J. Youngdahl, and J. R. Weertman: 'The strength of nanocrystalline metals with and without flaws', *Mater. Sci. Eng.: A*, 1997, **234-236**, 77-82.
176. A. H. Cottrell: 'Theory of brittle fracture in steel and similar metals', *Trans. Am. Inst. Metall. Eng.*, 1958, **212**, 192-203.
177. E. Smith and P. J. Worthington: 'The effect of orientation on the grain size dependence of the yield strength of metals', *Philos. Mag.*, 1964, **9**(98), 211-216.
178. A. Navarro and E. R. De Los Rios: 'An alternative model of the blocking of dislocations at grain boundaries', *Philos. Mag. A*, 1988, **57**(1), 37-42.
179. A. A. Nazarov: 'On the pile-up model of the grain size-yield stress relation for nanocrystals', *Scripta Mater.*, 1996, **34**(5), 697-701.
180. L. H. Friedman and D. C. Chrzan: 'Continuum analysis of dislocation pile-ups: influence of sources', *Philos. Mag. A*, 1998, **77**(5), 1185-1204.
181. J. C. M. Li: 'Petch relation and grain boundary sources', *Trans. Am. Inst. Metall. Eng.*, 1963, **227**(1), 239.
182. V. Bata and E. V. Pereloma: 'An alternative physical explanation of the Hall–Petch relation', *Acta Mater.*, 2004, **52**(3), 657-665.
183. J. A. Wert: 'Comments on "An alternative physical explanation of the Hall–Petch relation"', *Scripta Mater.*, 2004, **50**(12), 1487-1490.
184. V. G. Gavriljuk: 'Comment on "Alternative physical explanation of the Hall–Petch relation"', *Scripta Mater.*, 2005, **52**(9), 951-953.
185. M. F. Ashby: 'The deformation of plastically non-homogeneous materials', *Philos. Mag.*, 1970, **21**(170), 399-424.
186. A. W. Thompson, M. I. Baskes, and W. F. Flanagan: 'The dependence of polycrystal work hardening on grain size', *Acta Metall.*, 1973, **21**(7), 1017-1028.
187. M. A. Meyers and E. Ashworth: 'A model for the effect of grain size on the yield stress of metals', *Philos. Mag. A*, 1982, **46**(5), 737-759.

188. H. Conrad: 'Effect of grain size on the lower yield and flow stress of iron and steel', *Acta Metall.*, 1963, **11**(1), 75-77.
189. J. D. Meakin and N. J. Petch: 'Strain-hardening of polycrystals: The alpha-brasses', *Philos. Mag.*, 1974, **29**(5), 1149-1156.
190. L. E. Murr: 'Yielding and grain-boundary ledges: Some comments on the Hall-Petch relation', *Appl. Phys. Let.*, 1974, **24**(11), 533-536.
191. J. P. Bailon, A. Loyer, and J. M. Dorlot: 'The relationships between stress, strain, grain size and dislocation density in Armco iron at room temperature', *Mater. Sci. Eng.*, 1971, **8**(5), 288-298.
192. J. W. Edington and R. E. Smallman: 'The relationship between flow stress and dislocation density in deformed vanadium', *Acta Metall.*, 1964, **12**(12), 1313-1328.
193. W. Boas and M. E. Hargreaves: 'On the inhomogeneity of plastic deformation in the crystals of an aggregate', *Proc. Royal Soc. A*, 1948, **193**(1032), 89-97.
194. W. Boas and G. J. Ogilvie: 'The plastic deformation of a crystal in a polycrystalline aggregate', *Acta Metall.*, 1954, **2**(5), 655-659.
195. L. E. Murr and S. S. Hecker: 'Quantitative evidence for dislocation emission from grain boundaries', *Scripta Metall.*, 1979, **13**(3), 167-171.
196. H. Margolin and M. S. Stanescu: 'Polycrystalline strengthening', *Acta Metall.*, 1975, **23**(12), 1411-1418.
197. H. H. Fu, D. J. Benson, and M. A. Meyers: 'Analytical and computational description of effect of grain size on yield stress of metals', *Acta Mater.*, 2001, **49**(13), 2567-2582.
198. J. Jiang, T. B. Britton, and A. J. Wilkinson: 'Evolution of dislocation density distributions in copper during tensile deformation', *Acta Mater.*, 2013, **61**(19), 7227-7239.
199. W. M. Baldwin: 'Yield strength of metals as a function of grain size', *Acta Metallurgica*, 1958, **6**(2), 139-141.
200. T. Christman: 'Grain boundary strengthening exponent in conventional and ultrafine microstructures', *Scripta Metallurgica et Materialia*, 1993, **28**(12), 1495-1500.
201. J. P. Hirth: 'The influence of grain boundaries on mechanical properties', *Metallurgical Transactions*, 1972, **3**(12), 3047-3067.
202. D. J. Dunstan and A. J. Bushby: 'Grain size dependence of the strength of metals: the Hall–Petch effect does not scale as the inverse square root of grain size', *International Journal of Plasticity*, 2014, **53**, 56-65.
203. W. L. Bragg: 'A theory of the strength of metals', *Nature*, 1942, **149**, 511-513.
204. U. F. Kocks: 'The relation between polycrystal deformation and single-crystal deformation', *Metallurgical and Materials Transactions*, 1970, **1**(5), 1121-1143.
205. G. Taylor: 'Thermally-activated deformation of BCC metals and alloys', *Prog. Mater. Sci.*, 1992, **36**, 29-61.
206. J. W. Christian: 'Some surprising features of the plastic deformation of body-centered cubic metals and alloys', *Metall. Trans. A*, 1983, **14**(7), 1237-1256.
207. C. A. Schuh, T. G. Nieh, and H. Iwasaki: 'The effect of solid solution W additions on the mechanical properties of nanocrystalline Ni', *Acta Mater.*, 2003, **51**(2), 431-443.
208. J. M. Rosenberg and H. R. Piehler: 'Calculation of the Taylor factor and lattice rotations for bcc metals deforming by pencil glide', *Metall. Trans.*, 1971, **2**(1), 257-259.
209. B. L. Mordike and P. Haasen: 'The influence of temperature and strain rate on the flow stress of alpha-iron single crystals', *Philos. Mag.*, 1962, **7**(75), 459-474.
210. N. P. Allen, B. E. Hopkins, and J. E. McLennan: 'The tensile properties of single crystals of high-purity iron at temperatures from 100 to -253 °C', *Proc. Royal Soc. A*, 1956, **234**(1197), 221-246.
211. W. A. Spitzig and A. S. Keh: 'Orientation dependence of the strain-rate sensitivity and thermally activated flow in iron single crystals', *Acta Metall.*, 1970, **18**(9), 1021-1033.
212. R. P. Steijn and R. M. Brick: 'Flow and fracture of single crystals of high purity ferrite', *Trans. Am. Soc. Metall.*, 1954, **46**, 1406-1448.

213. F. Guiu and P. L. Pratt: 'The effect of orientation on the yielding and flow of molybdenum single crystals', *Phys. Stat. Sol. (b)*, 1966, **15**(2), 539-552.
214. H. J. Kauemann: 'Plasticity of molybdenum single crystals at helium temperature', *Phys. Stat. Sol. (a)*, 1981, **65**(1), 53-58.
215. R. T. Sato and A. K. Mukherjee: 'The asymmetric temperature dependence of yield stress in tantalum single crystals at low temperatures', *Mater. Sci. Eng.*, 1971, **8**(2), 74-82.
216. B. L. Mordike: 'Plastic deformation of zone refined tantalum single crystals', *Z. Metallk.*, 1962, **53**(9), 586-592.
217. J. Bressers, M. Heerschap, and P. De Meester: 'Deformation properties of vanadium single crystals', *J. Less Common Met.*, 1970, **22**(3), 321-326.
218. T. E. Mitchell, R. J. Fields, and R. L. Smialek: 'Three-stage hardening in vanadium single crystals', *J. Less Common Met.*, 1970, **20**(2), 167-170.
219. M. S. Wechsler, R. P. Tucker, and R. Bode: 'Radiation hardening in single crystal niobium—The temperature dependence of yielding', *Acta Metall.*, 1969, **17**(5), 541-551.
220. U. F. Kocks: 'The relation between polycrystal deformation and single-crystal deformation', *Metall. Mater. Trans.*, 1970, **1**(5), 1121-1143.
221. R. W. K. Honeycombe: 'The plastic deformation of metals'; 1975, London, Edward Arnold.
222. U. F. Kocks: 'Laws for work-hardening and low-temperature creep', *J. Eng. Mater. Technol.*, 1976, **98**(1), 76-85.
223. L. E. Murr: 'Interfacial phenomena in metals and alloys'; 1975, Boston, MA, Addison-Wesley.
224. D. Tabor: 'The hardness of metals'; 1951, Oxford, Clarendon Press.
225. Z. C. Szkopiak: 'Interstitial solute pick-up in annealed niobium and the Hall-Petch plot', *J. Less Common Met.*, 1972, **26**(1), 19-24.
226. M. A. Meyers, A. Mishra, and D. J. Benson: 'Mechanical properties of nanocrystalline materials', *Progress in Materials Science*, 2006, **51**(4), 427-556.
227. M. Dao, L. Lu, R. J. Asaro, J. T. M. De Hosson, and E. Ma: 'Toward a quantitative understanding of mechanical behavior of nanocrystalline metals', *Acta Materialia*, 2007, **55**(12), 4041-4065.
228. F. A. McClintock and A. S. Argon: 'Mechanical behavior of materials'; 1966, Boston, MA, Addison-Wesley.
229. R. C. Hugo, H. Kung, J. R. Weertman, R. Mitra, J. A. Knapp, and D. M. Follstaedt: 'In-situ TEM tensile testing of DC magnetron sputtered and pulsed laser deposited Ni thin films', *Acta Mater.*, 2003, **51**(7), 1937-1943.
230. K. S. Kumar, S. Suresh, M. F. Chisholm, J. A. Horton, and P. Wang: 'Deformation of electrodeposited nanocrystalline nickel', *Acta Mater.*, 2003, **51**(2), 387-405.
231. K. M. Youssef, R. O. Scattergood, K. L. Murty, J. A. Horton, and C. C. Koch: 'Ultrahigh strength and high ductility of bulk nanocrystalline copper', *Appl. Phys. Let.*, 2005, **87**(9).
232. C. J. Youngdahl, J. R. Weertman, R. C. Hugo, and H. H. Kung: 'Deformation behavior in nanocrystalline copper', *Scripta Mater.*, 2001, **44**(8), 1475-1478.
233. K. Jonnalagadda, N. Karanjgaokar, I. Chasiotis, J. Chee, and D. Peroulis: 'Strain rate sensitivity of nanocrystalline Au films at room temperature', *Acta Mater.*, 2010, **58**(14), 4674-4684.
234. M. A. Haque and M. T. A. Saif: 'Deformation mechanisms in free-standing nanoscale thin films: A quantitative in situ transmission electron microscope study', *Proc. Natl Acad. Sci.*, 2004, **101**(17), 6335-6340.
235. L. Wang, Z. Zhang, E. Ma, and X. D. Han: 'Transmission electron microscopy observations of dislocation annihilation and storage in nanograins', *Appl. Phys. Let.*, 2011, **98**(5), 51905.
236. G. M. Cheng, W. W. Jian, W. Z. Xu, H. Yuan, P. C. Millett, and Y. T. Zhu: 'Grain size effect on deformation mechanisms of nanocrystalline BCC metals', *Mater. Res. Let.*, 2013, **1**(1), 26-31.
237. M. Hommel and O. Kraft: 'Deformation behavior of thin copper films on deformable substrates', *Acta Mater.*, 2001, **49**(19), 3935-3947.
238. R. J. Asaro, P. Krysl, and B. Kad: 'Deformation mechanism transitions in nanoscale FCC metals', *Philos. Mag. Let.*, 2003, **83**(12), 733-743.

239. R. J. Asaro and S. Suresh: 'Mechanistic models for the activation volume and rate sensitivity in metals with nanocrystalline grains and nano-scale twins', *Acta Mater.*, 2005, **53**(12), 3369-3382.
240. P. Gu, M. Dao, R. J. Asaro, and S. Suresh: 'A unified mechanistic model for size-dependent deformation in nanocrystalline and nanotwinned metals', *Acta Mater.*, 2011, **59**(18), 6861-6868.
241. P. Gu, B. K. Kad, and M. Dao: 'Revisiting the intra-granular dislocation extension model for flow stress in nanocrystalline metals', *Philos. Mag. Let.*, 2012, **92**(3), 111-121.
242. A. S. Argon and S. Yip: 'The strongest size', *Philos. Mag. Let.*, 2006, **86**(11), 713-720.
243. J. Schiøtz and K. W. Jacobsen: 'A maximum in the strength of nanocrystalline copper', *Science*, 2003, **301**(5638), 1357-1359.
244. J. Schiøtz, T. Vegge, F. D. Di Tolla, and K. W. Jacobsen: 'Atomic-scale simulations of the mechanical deformation of nanocrystalline metals', *Phys. Rev. B*, 1999, **60**(17), 11971.
245. V. Yamakov, D. Wolf, S. R. Phillpot, A. K. Mukherjee, and H. Gleiter: 'Deformation-mechanism map for nanocrystalline metals by molecular-dynamics simulation', *Nature Mater.*, 2004, **3**(1), 43-47.
246. J. R. Trelewicz and C. A. Schuh: 'The Hall–Petch breakdown in nanocrystalline metals: a crossover to glass-like deformation', *Acta Mater.*, 2007, **55**(17), 5948-5958.
247. W. Qin, Z. Chen, P. Huang, and Y. Zhuang: 'Dislocation pileups in nanocrystalline materials', *J. of Alloys and Compounds*, 1999, **289**(1), 285-288.
248. T. G. Nieh and J. Wadsworth: 'Hall-Petch relation in nanocrystalline solids', *Scripta Metall. Mater.*, 1991, **25**(4), 955-958.
249. C. E. Carlton and P. J. Ferreira: 'What is behind the inverse Hall–Petch effect in nanocrystalline materials?', *Acta Mater.*, 2007, **55**(11), 3749-3756.
250. J. E. Carsley, J. Ning, W. W. Milligan, S. A. Hackney, and E. C. Aifantis: 'A simple, mixtures-based model for the grain size dependence of strength in nanophase metals', *Nanostruc. Mater.*, 1995, **5**(4), 441-448.
251. H. S. Kim: 'A composite model for mechanical properties of nanocrystalline materials', *Scripta Mater.*, 1998, **39**(8), 1057-1061.
252. P. Barai and G. J. Weng: 'Mechanics of very fine-grained nanocrystalline materials with contributions from grain interior, GB zone, and grain-boundary sliding', *Int. J. Plast.*, 2009, **25**(12), 2410-2434.
253. G. J. Fan, H. Choo, P. K. Liaw, and E. J. Lavernia: 'A model for the inverse Hall–Petch relation of nanocrystalline materials', *Mater. Sci. Eng.: A*, 2005, **409**(1), 243-248.
254. M. Huang, O. Bouaziz, and S. van der Zwaag: 'Modelling the strongest grain size in nanocrystalline FCC metals', *Mater. Let.*, 2011, **65**(19), 3128-3130.
255. F. A. Mohamed and H. Yang: 'Deformation mechanisms in nanocrystalline materials', *Metall. Mater. Trans. A*, 2010, **41**(4), 823-837.
256. X. Zhang and K. E. Aifantis: 'Interpreting the softening of nanomaterials through gradient plasticity', *J. Mater. Res.*, 2011, **26**(11), 1399-1405.
257. H. W. Song, S. R. Guo, and Z. Q. Hu: 'A coherent polycrystal model for the inverse Hall-Petch relation in nanocrystalline materials', *Nanostruc. Mater.*, 1999, **11**(2), 203-210.
258. S. Takeuchi: 'The mechanism of the inverse Hall-Petch relation of nanocrystals', *Scripta Mater.*, 2001, **44**(8), 1483-1487.
259. A. A. Fedorov, M. Y. Gutkin, and I. A. Ovid'ko: 'Transformations of grain boundary dislocation pile-ups in nano-and polycrystalline materials', *Acta Mater.*, 2003, **51**(4), 887-898.
260. A. A. Fedorov, M. Y. Gutkin, and I. A. Ovid'ko: 'Triple junction diffusion and plastic flow in fine-grained materials', *Scripta Mater.*, 2002, **47**(1), 51-55.
261. H. S. Kim and Y. Estrin: 'Phase mixture modeling of the strain rate dependent mechanical behavior of nanostructured materials', *Acta Mater.*, 2005, **53**(3), 765-772.
262. N. Wang, Z. Wang, K. T. Aust, and U. Erb: 'Effect of grain size on mechanical properties of nanocrystalline materials', *Acta Metall. Mater.*, 1995, **43**(2), 519-528.

263. A. H. Chokshi: 'An analysis of creep deformation in nanocrystalline materials', *Scripta Mater.*, 1996, **34**(12), 1905-1910.
264. A. H. Chokshi: 'Unusual stress and grain size dependence for creep in nanocrystalline materials', *Scripta Mater.*, 2009, **61**(1), 96-99.
265. D. S. Gianola, D. H. Warner, J. F. Molinari, and K. J. Hemker: 'Increased strain rate sensitivity due to stress-coupled grain growth in nanocrystalline Al', *Scripta Mater.*, 2006, **55**(7), 649-652.
266. Y. M. Wang, A. V. Hamza, and E. Ma: 'Temperature-dependent strain rate sensitivity and activation volume of nanocrystalline Ni', *Acta Mater.*, 2006, **54**(10), 2715-2726.
267. M. Park and C. A. Schuh: 'Accelerated sintering in phase-separating nanostructured alloys', *Nature Comm.*, 2015, **6**.
268. T. Chookajorn, H. A. Murdoch, and C. A. Schuh: 'Design of stable nanocrystalline alloys', *Science*, 2012, **337**(6097), 951-954.
269. S. J. Dillon, M. Tang, W. C. Carter, and M. P. Harmer: 'Complexion: A new concept for kinetic engineering in materials science', *Acta Mater.*, 2007, **55**(18), 6208-6218.
270. L. Lu, X. Chen, X. Huang, and K. Lu: 'Revealing the maximum strength in nanotwinned copper', *Science*, 2009, **323**(5914), 607-610.
271. K. Lu, L. Lu, and S. Suresh: 'Strengthening materials by engineering coherent internal boundaries at the nanoscale', *Science*, 2009, **324**(5925), 349-352.
272. M. A. Meyers, O. Vöhringer, and V. A. Lubarda: 'The onset of twinning in metals: a constitutive description', *Acta Mater.*, 2001, **49**(19), 4025-4039.
273. R. W. Armstrong and P. J. Worthington: 'A constitutive relation for deformation twinning in body centered cubic metals'; 1973, New York, Plenum Press.
274. A. Ghaderi and M. R. Barnett: 'Sensitivity of deformation twinning to grain size in titanium and magnesium', *Acta materialia*, 2011, **59**(20), 7824-7839.

Figure and Table Captions

Figure 1: Aggregated Hall-Petch data for each of the BCC metals as well as best fits to the data using equation (1). The closed points indicate Vickers and nanoindentation hardness measurements that were divided by a Tabor factor of 3 while the open points indicate yield strengths measured using compression or tension tests. The Refs. included in a-g) are as follows: a) 12-18; b) 19-29; c) 14, 30-37; d) 38-56; e) 57-60; f) 61-66; and g) 67, 68.

Figure 2: Aggregated Hall-Petch data for each of the FCC metals as well as best fits to the data using equation (1). The closed points indicate Vickers and nanoindentation hardness measurements that were divided by a Tabor factor of 3 while the open points indicate yield strengths measured using compression or tension tests. The Refs. included in a-e) are as follows: a) 69-86; b) 87-91; c) 92-95; d) 96-107; and e) 8, 108-122.

Figure 3: Aggregated Hall-Petch data for each of the HCP metals as well as best fits to the data using equation (1). The closed points indicate Vickers and nanoindentation hardness measurements that were divided by a Tabor factor of 3 while the open points indicate yield strengths measured using compression or tension tests. The Refs. included in a-h) are as follows: a) 123-132; b) 133-137; c) 138; d) 139-144; e) 6, 145-156; f) 7, 10, 157-163; g) 164-171; and h) 172-174.

Table 1: Summary of results from Hall-Petch studies on pure metals.

Table 2: Summary of grain size strengthening models.

Figure 4: $k/(Gb^{1/2})$ as a function of plastic strain for several FCC, BCC, and HCP metals.

Figure 5: Aggregated grain size strengthening data for Ni as well as best fits using equation (9) to the results from the individual studies.

Table 3: *n* and *k* values from best fits using equation (9) to each metal's aggregated grain size strengthening data.

Figure 6: Testing temperature versus $M_{ave}\tau_0$ from tension tests on single crystals and σ_0 from fits to yield stress measurements using the Hall-Petch equation. We used M_{ave} = 2.7 which is appropriate for BCC polycrystals that exhibit pencil glide and have no texture.[208] The close correspondence between $M_{ave}\tau_0$ and σ_0 supports equation (11a). The large and rapid increase in both $M_{ave}\tau_0$ and σ_0 with decreasing temperature reflects the BCC metals' large, temperature-sensitive Peierls-Nabarro stress. The single crystal data in a-e) are from the following Refs.: a) 209-212; b) 213, 214; c) 215, 216; d) 217, 218; and e) 219.

Figure 7: a) Increase in several BCC metals' σ_0/G with plastic strain at room temperature. b,c) Increase in several FCC metals' σ_0/G with plastic strain at room temperature and 77 K, respectively. Note the close resemblance of these results to the increase in the flow stress of single crystal test specimens oriented for multislip during tension or compression testing. The material and testing parameters affecting the normalized rate of work-hardening of single crystals – crystal structure, stacking fault energy (SFE),[223] temperature – have the same effect on σ_0/G's strain dependence.

Figure 8: Independent fits using equation (1) to the niobium grain size strengthening data from Refs. 19, 20, 23, 24, 27, 29.

Table 4: Interstitial content and corresponding solid solution strengthening increment in the Nb studies shown in Figure 7. The solid solution strengthening increments for oxygen and nitrogen are 0.19 and 0.41 MPa/ppm, respectively.[225]

Figure 9: Chromium grain size strengthening data from Refs. 59, 60 as well as best fits using equation (1) to each study's data.

Supplementary Material 1: Summary of the grain size strengthening data shown in Figures 1-3.

Supplementary Material 2: Summary of the experimental details from each of the Hall-Petch studies cited herein. This table includes the specimen purity, the processing techniques used to prepare the test specimens, the mechanical test method, and the technique used to measure the grain size.